UC Berkeley
UC Berkeley Previously Published Works

Title

Specific α-Arrestins Negatively Regulate Saccharomyces cerevisiae Pheromone Response by Down-Modulating the G-Protein-Coupled Receptor Ste2

Authors

Alvaro, Christopher G
O'Donnell, Allyson F
Prosser, Derek C
et al.

Specific α-Arrestins Negatively Regulate *Saccharomyces cerevisiae* Pheromone Response by Down-Modulating the G-Protein-Coupled Receptor Ste2

Christopher G. Alvaro,[a] Allyson F. O'Donnell,[a,b] Derek C. Prosser,[c] Andrew A. Augustine,[d] Aaron Goldman,[e] Jeffrey L. Brodsky,[d] Martha S. Cyert,[e] Beverly Wendland,[c] Jeremy Thorner[a]

Division of Biochemistry, Biophysics and Structural Biology, Department of Molecular and Cell Biology, University of California, Berkeley, California, USA[a]; Department of Cell Biology, School of Medicine, University of Pittsburgh, Pittsburgh, Pennsylvania, USA[b]; Department of Biology, The Johns Hopkins University, Baltimore, Maryland, USA[c]; Department of Biological Sciences, University of Pittsburgh, Pittsburgh, Pennsylvania, USA[d]; Department of Biology, Stanford University, Stanford, California, USA[e]

G-protein-coupled receptors (GPCRs) are integral membrane proteins that initiate responses to extracellular stimuli by mediating ligand-dependent activation of cognate heterotrimeric G proteins. In yeast, occupancy of GPCR Ste2 by peptide pheromone α-factor initiates signaling by releasing a stimulatory Gβγ complex (Ste4-Ste18) from its inhibitory Gα subunit (Gpa1). Prolonged pathway stimulation is detrimental, and feedback mechanisms have evolved that act at the receptor level to limit the duration of signaling and stimulate recovery from pheromone-induced G$_1$ arrest, including upregulation of the expression of an α-factor-degrading protease (Bar1), a regulator of G-protein signaling protein (Sst2) that stimulates Gpa1-GTP hydrolysis, and Gpa1 itself. Ste2 is also downregulated by endocytosis, both constitutive and ligand induced. Ste2 internalization requires its phosphorylation and subsequent ubiquitinylation by membrane-localized protein kinases (Yck1 and Yck2) and a ubiquitin ligase (Rsp5). Here, we demonstrate that three different members of the α-arrestin family (Ldb19/Art1, Rod1/Art4, and Rog3/Art7) contribute to Ste2 desensitization and internalization, and they do so by discrete mechanisms. We provide genetic and biochemical evidence that Ldb19 and Rod1 recruit Rsp5 to Ste2 via PPXY motifs in their C-terminal regions; in contrast, the arrestin fold domain at the N terminus of Rog3 is sufficient to promote adaptation. Finally, we show that Rod1 function requires calcineurin-dependent dephosphorylation.

For survival, eukaryotic cells sense and respond to changes in external conditions using, in many cases, a G-protein-coupled receptor (GPCR) (1, 2). Most clinically used pharmaceuticals act on GPCRs (3, 4). After an initial response, cells normally adapt by becoming desensitized to the stimulus, whereas chronic GPCR action can lead to inflammation and other pathophysiologies (5, 6). Thus, the mechanisms underlying both GPCR signal transmission and its attenuation have important medical implications.

In *Saccharomyces cerevisiae*, GPCR Ste2 in the plasma membrane (PM) of a *MAT***a** haploid cell binds α-factor (a 13-residue peptide) secreted by a *MAT*α haploid cell, and a *MAT*α haploid uses GPCR Ste3 to bind **a**-factor (a 12-residue prenylated peptide) released by a *MAT***a** haploid (7). Engagement of these receptors by these ligands (mating pheromones) initiates a mitogen-activated protein kinase (MAPK) cascade. The activated MAPK evokes transcriptional and morphological responses that arrest cell growth in the G$_1$ phase of the cell cycle and convert the cells to gametes, which conjugate (mate) to form a *MAT***a**/*MAT*α diploid (8, 9). Genetic and molecular analysis of this system has established many important concepts in GPCR-initiated signaling and its regulation (10–13).

Hyperactivation or prolonged signaling through the mating pheromone response pathway can cause cell death (14). To avoid this, α-factor also induces feedback mechanisms that downregulate signaling in *MAT***a** cells. Paramount among these adaptation processes is upregulation of expression of genes for a variety of negative regulators, such as *MSG5*, which encodes a phosphoprotein phosphatase that deactivates the terminal MAPK (Fus3) of the pathway (15, 16). However, induced negative regulators also include factors that desensitize the pathway far upstream by acting

on α-factor, its receptor, or the associated heterotrimeric G protein, preventing further GPCR-initiated signaling. For example, *BAR1* encodes a protease that cleaves α-factor into two inactive fragments (17, 18). *SST2* encodes the first regulator of G-protein signaling (RGS) identified (7, 19, 20). Binding of its N-terminal DEP domains to the cytosolic tail of Ste2 (21) delivers Sst2 to the PM. Thus, its C-terminal RGS domain is positioned to stimulate conversion of PM-localized GTP-bound Gpa1 back to its GDP state (22). GDP-Gpa1 then reassociates with and blocks downstream signaling by the Ste4-Ste18 complex (23, 24), which is also PM anchored via S-palmitoylation and S-farnesylation of Ste18 (25, 26). Recoupling and squelching of Gβγ function is further promoted by mass action, because *GPA1* is upregulated in response to pheromone (27), concomitant with an enhanced rate of its N-myristoylation (28), a posttranslational modification essential for Gpa1 PM targeting, coupling to Gβγ, and association with the receptor (23, 29).

Termination of an agonist-initiated GPCR-mediated signal is also thought to involve ligand-induced receptor endocytosis (30,

31). It has been known for decades that both Ste2 and Ste3 undergo constitutive internalization at a basal rate and that endocytosis is stimulated upon binding of the cognate pheromone (32–36). Pheromone binding causes a conformational change that promotes phosphorylation of the Ste2 and Ste3 C termini (37–39), mediated by PM-anchored casein kinase I isoforms (Yck1 and Yck2) (21, 40). Phosphorylation is a prelude to receptor ubiquitinylation (39, 41) by a PM-associated HECT domain-containing ubiquitin ligase (E3), Rsp5 (42–44) (the mammalian ortholog is NEDD4L [45]). Ubiquitin attachment targets the receptors for clathrin-mediated internalization (46, 47). The resulting endosomes are delivered to the vacuole (equivalent to a mammalian lysosome) where the receptor is degraded (48, 49).

Subsequent studies have provided more detailed analysis of spatiotemporal aspects of Ste2 (50, 51) and Ste3 (52, 53) internalization and better delineated the phosphorylation and ubiquitinylation sites (54, 55). However, how Rsp5 recognizes and is recruited to these GPCRs to catalyze ubiquitinylation remained unresolved. Discovery in yeast of a protein family, called the α-arrestins, that serve as adaptors for Rsp5-dependent ubiquitinylation and internalization of nutrient permeases provided a clue (56–58). The *S. cerevisiae* genome encodes 14 currently recognized members of the α-arrestin family (57–60). The name derives from homology of their N-terminal domains to a fold found in mammalian arrestin and β-arrestins (56, 61), first identified and implicated in blocking signaling by rhodopsin (62) and the β-adrenergic receptor (63), respectively.

As described here, we found that three different α-arrestins, Ldb19/Art1, Rod1/Art4, and Rog3/Art7, have overlapping functions and contribute to Ste2 internalization and *MAT***a** cell recovery from pheromone-induced G_1 arrest. Surprisingly, the modes of action of these α-arrestins are distinct. Ldb19 plays a role primarily in basal turnover of Ste2, whereas Rod1 and Rog3 contribute to desensitization of the agonist-occupied receptor. Although paralogous on the basis of primary sequence, Rod1 and Rog3 act by different mechanisms; Rod1 is obligatorily Rsp5 dependent, but Rog3 is not. Moreover, Rod1 (but not Rog3) function during Ste2 downregulation requires calcineurin (CN)-dependent dephosphorylation. Together, our studies extend the function of α-arrestins to another class of polytopic membrane protein and demonstrate discrete actions of α-arrestin family members whose functions previously have been enigmatic.

MATERIALS AND METHODS

Strains and growth conditions. Yeast strains (Table 1) were grown at 30°C in either rich (YPD) or synthetic complete (SC) medium containing 2% glucose (unless another carbon source is specified) and with appropriate nutrients to maintain selection for plasmids, if present (64). Standard genetic methods were used for strain construction (65).

Plasmids. Plasmids (Table 2) were constructed using standard procedures (66). DNA amplification by PCR (66) employed Phusion DNA polymerase (New England BioLabs, Ipswich, MA), and all constructs were verified by sequencing. Site-directed mutagenesis (67) was carried out using the same DNA polymerase and QuikChange methodology (New England BioLabs) according to the manufacturer's instructions.

Pheromone-imposed growth arrest. Response to α-factor was assessed by an agar diffusion (halo) bioassay essentially as described previously (37). In brief, cells (~10^5) were plated in top agar on solid YPD or SC medium as appropriate. On the resulting surface were laid sterile cellulose filter disks, onto which an aliquot (typically, 15 μl) of an aqueous solution (1 mg/ml) of α-factor (GeneScript, Piscataway, NJ) had been

aseptically spotted, and the plates were incubated at 30°C for 2 to 4 days. To induce α-arrestin overexpression, strains containing the tripartite *S. cerevisiae* Gal4-human estrogen receptor-herpes simplex virus transactivator VP16 fusion protein (Gal4-ER-VP16 or GEV) (68, 69) and *URA3*-marked multicopy (2μm DNA) plasmids expressing from the *GAL1,10* promoter the α-arrestin of interest (as a fusion to the C terminus of glutathione *S*-transferase [GST]) were grown to mid-exponential phase. The cultures were then treated with β-estradiol (20 μM final concentration) for 3 h and plated using top agar containing 200 nM β-estradiol. Samples of the same cultures were analyzed by immunoblotting (see below) to confirm α-arrestin expression.

Mating pathway activation. As one measure of pathway activation, the level of dually phosphorylated Fus3 was assessed as follows. Strains of interest carrying a *bar1*Δ mutation were grown in YPD to mid-exponential phase, a sample was removed (zero time point), and immediately thereafter the culture was treated with α-factor (15 nM final concentration). Additional samples of equivalent numbers of cells then were removed at 10, 30, 60, and 90 min, harvested by rapid sedimentation in a microcentrifuge, and immediately frozen in liquid N_2. The cell pellets were thawed on ice, and whole-cell protein extracts were prepared by alkaline lysis followed by collection of total protein by trichloroacetic acid (TCA) precipitation (70, 71). Protein precipitates were solubilized in SDS-urea gel sample buffer (5% SDS, fresh 8 M urea, 1% β-mercaptoethanol, 0.1 mM EDTA, 40 mM Tris-HCl [pH 6.8]) with 0.1% bromophenol blue, heated at 37°C for 15 min, resolved in a slab gel by SDS-PAGE (72), and analyzed by immunoblotting.

As an independent measure of pathway activation, induction of an integrated single-copy *FUS1$_{prom}$*-enhanced green fluorescent protein (eGFP) reporter (73) was monitored. Strains of interest carrying a *bar1*Δ mutation and also containing integrated *FUS1$_{prom}$*-eGFP were constructed (Table 1). These cells were grown to mid-exponential phase and treated with 15 nM α-factor for 2 h, and the level of GFP expression was quantified by flow cytometry using a Beckman-Coulter FC-500 analyzer. The resulting data were analyzed using FlowJo software (Tree Star, Inc.).

Immunoblotting. Equal numbers of cells from mid-exponential-phase cultures were collected by centrifugation and lysed, and total protein was collected and resolved by SDS-PAGE as described above. The proteins in the resulting slab gels were transferred electrophoretically to nitrocellulose sheets (74) using a semidry transfer apparatus (Transblot SD; Bio-Rad, Inc.). After blocking with carrier protein (75), the filters were incubated (generally for several h at room temperature or overnight at 4°C) with the following primary antibodies, as appropriate: rabbit polyclonal anti-GST (Sigma), rabbit polyclonal anti-phospho-extracellular signal-regulated kinase (anti-phospho-ERK; Cell Signaling), goat polyclonal anti-Fus3 (Santa Cruz), mouse monoclonal anti-HA (12CA5; Roche), mouse monoclonal antiubiquitin (P4D1; Santa Cruz), and, as loading control, rabbit polyclonal anti-Pgk1 (76). The resulting immune complexes were then detected by incubation, as appropriate, with infrared dye (IRDye 680/800)-labeled secondary antibodies, namely, goat anti-mouse IgG, goat anti-rabbit IgG, or donkey anti-goat antibody (all from Li-Cor, Lincoln, NE), followed by visualization using an infrared imager (Odyssey; Li-Cor). In experiments assessing the ratio of phosphorylated to total Fus3, band intensities were quantified for each time point using ImageJ software (National Institutes of Health). Alternatively, in some experiments, to monitor GFP-tagged proteins and after blocking with SuperBlock (Thermo Scientific, Rockford, IL), filters were incubated with rabbit polyclonal anti-GFP antibodies (Invitrogen), and the resulting immune complexes were detected with horseradish peroxidase-conjugated donkey anti-rabbit IgG antibodies (GE Healthcare). To monitor GST-tagged proteins, the complexes were incubated with mouse monoclonal anti-GST antibodies (Covance) and detected with horseradish peroxidase-conjugated sheep anti-mouse IgG antibodies (GE Healthcare). The bound immune complexes were then visualized by chemiluminescence using either ECL Western blotting substrate (Pierce) or SuperSignal West

TABLE 1 Yeast strains used in this study

Strain	Genotype	Reference or source
BY4741	*MAT**a** leu2Δ0 ura3Δ0 his3Δ1 met15Δ0*	Yeast deletion collection (Open Biosystems, Inc.)
9arrΔ (EN60)	*ecm21Δ::KANMX csr2Δ::KANMX bsd2Δ rog3Δ::NATMX rod1Δ ygr068cΔ aly2Δ aly1Δ ldb19Δ ylr392cΔ::HIS3 his3 leu2Δ0 ura3Δ0*	58
ldb19Δ	*MAT**a** leu2Δ0 ura3Δ0 his3Δ1 met15Δ0 ldb19Δ::KANMX4*	Yeast deletion collection (Open Biosystems, Inc.)
rod1Δ rog3Δ (JT5858)	*MAT**a** leu2Δ0 ura3Δ0 his3Δ1 met15Δ0 rod1Δ::KANMX4 rog3Δ::KANMX4*	This study
aly1Δ aly2Δ (D2-6A)	*MAT**a** leu2Δ0 ura3Δ0 his3Δ1 met15Δ0 aly1Δ::KANMX4 aly2Δ::KANMX4*	86
ecm21Δ csr2Δ (JT6751)	*MAT**a** leu2Δ0 ura3Δ0 his3Δ1 met15Δ0 ecm21Δ::KANMX4 csr2Δ::KANMX4*	This study
art5Δ rim8Δ (JT5860)	*MAT**a** leu2Δ0 ura3Δ0 his3Δ1 met15Δ0 art5Δ::KANMX4 rim8Δ::KANMX4*	This study
art10Δ	*MAT**a** leu2Δ0 ura3Δ0 his3Δ1 met15Δ0 art10Δ::KANMX4*	Yeast deletion collection (Open Biosystems, Inc.)
rod1Δ rog3Δ ldb19Δ (JT6675)	*MAT**a** leu2Δ0 ura3Δ0 his3Δ1 met15Δ0 rod1Δ::KANMX4 rog3Δ::KANMX4 ldb19Δ::NATMX*	This study
bar1Δ (JT5915)	*MAT**a** leu2Δ0 ura3Δ0 his3Δ1 met15Δ0 bar1Δ::CgLEU2*	This study
ldb19Δ bar1Δ (JT5916)	*MAT**a** leu2Δ0 ura3Δ0 his3Δ1 met15Δ0 ldb19Δ::KANMX4 bar1Δ::CgLEU2*	This study
rod1Δ rog3Δ bar1Δ (JT5917)	*MAT**a** leu2Δ0 ura3Δ0 his3Δ1 met15Δ0 rod1Δ::KANMX4 rog3Δ::KANMX4 bar1Δ::CgLEU2*	This study
rod1Δ rog3Δ ldb19Δ bar1Δ (JT6674)	*MAT**a** leu2Δ0 ura3Δ0 his3Δ1 met15Δ0 rod1Δ::KANMX4 rog3Δ::KANMX4 ldb19Δ::NATMX bar1Δ::CgLEU2*	This study
sst2Δ (JT6755)	*MAT**a** leu2Δ0 ura3Δ0 his3Δ1 met15Δ0 sst2Δ::SpHIS5*	This study
ldb19Δ sst2Δ (JT6660)	*MAT**a** leu2Δ0 ura3Δ0 his3Δ1 met15Δ0 ldb19Δ::KANMX4 sst2Δ::SpHIS5*	This study
rod1Δ rog3Δ sst2Δ (JT6702)	*MAT**a** leu2Δ0 ura3Δ0 his3Δ1 met15Δ0 rod1Δ::KANMX4 rog3Δ::KANMX4 sst2Δ::SpHIS5*	This study
rod1Δ rog3Δ ldb19Δ sst2Δ (JT6662)	*MAT**a** leu2Δ0 ura3Δ0 his3Δ1 met15Δ0 rod1Δ::KANMX4 rog3Δ::KANMX4 ldb19Δ::NATMX sst2Δ::SpHIS5*	This study
sst2Δ GEV (JT5919)[b]	*MAT**a** leu2Δ0 ura3Δ0 his3Δ1 met15Δ0 sst2Δ::SpHIS5 leu2Δ0::GEV::NATMX*	This study
rod1Δ rog3Δ ldb19Δ sst2Δ GEV (JT6716)	*MAT**a** leu2Δ0 ura3Δ0 his3Δ1 met15Δ0 rod1Δ::KANMX4 rog3Δ::KANMX4 ldb19Δ::NATMX sst2Δ::SpHIS5 leu2Δ0::GEV::NATMX*	This study
STE2-mCherry bar1Δ (JT6677)	*MAT**a** leu2Δ0 ura3Δ0 his3Δ1 met15Δ0 STE2-mCherry::URA3 bar1Δ::CgLEU2*	This study
STE2-mCherry ldb19Δ bar1Δ (JT6678)	*MAT**a** leu2Δ0 ura3Δ0 his3Δ1 met15Δ0 STE2-mCherry::URA3 ldb19Δ::KANMX4 bar1Δ::CgLEU2*	This study
STE2-mCherry rod1Δ rog3Δ bar1Δ (JT6679)	*MAT**a** leu2Δ0 ura3Δ0 his3Δ1 met15Δ0 STE2-mCherry::URA3 rod1Δ::KANMX4 rog3Δ::KANMX4 bar1Δ::CgLEU2*	This study
STE2-mCherry rod1Δ rog3Δ ldb19Δ bar1Δ (JT6680)	*MAT**a** leu2Δ0 ura3Δ0 his3Δ1 met15Δ0 STE2-mCherry::URA3 rod1Δ::KANMX4 rog3Δ::KANMX4 ldb19Δ::NATMX bar1Δ::CgLEU2*	This study
STE2-GFP (JT6757)	*MAT**a** leu2Δ0 ura3Δ0 his3Δ1 met15Δ0 STE2-GFP::HPH*	This study
9arrΔ STE2-GFP (JT6758)	*ecm21::G418 csr2::G418 bsd2 rog3::NATMX rod1 ygr068c aly2 aly1 ldb19 ylr392c::HIS his3 leu2Δ0 ura3Δ0 STE2-GFP::HPH*	This study
ldb19Δ STE2-GFP (JT6759)	*MAT**a** leu2Δ0 ura3Δ0 his3Δ1 met15Δ0 ldb19Δ::KANMX4 STE2-GFP::HPH*	This study
rod1Δ rog3Δ STE2-GFP (JT6760)	*MAT**a** leu2Δ0 ura3Δ0 his3Δ1 met15Δ0 STE2-GFP::HPH rod1Δ::KANMX4 rog3Δ::KANMX4*	This study
rod1Δ rog3Δ ldb19Δ STE2-GFP (JT6761)	*MAT**a** leu2Δ0 ura3Δ0 his3Δ1 met15Δ0 STE2-GFP::HPH rod1Δ::KANMX4 rog3Δ::KANMX4 ldb19Δ::NATMX*	This study
aly1Δ aly2Δ STE2-GFP (JT6762)	*MAT**a** leu2Δ0 ura3Δ0 his3Δ1 met15Δ0 STE2-GFP::HPH aly1Δ::KANMX4 aly2Δ::KANMX4*	This study
bar1Δ FUS1prom-eGFP (JT6686)[a]	*MAT**a** leu2Δ0 ura3Δ0 his3Δ1 met15Δ0 bar1Δ::URA3 FUS1prom-eGFP::LEU2*	This study
rod1Δ rog3Δ ldb19Δ bar1Δ FUS1prom-eGFP (JT6668)[a]	*MAT**a** leu2Δ0 ura3Δ0 his3Δ1 met15Δ0 rod1Δ::KANMX4 rog3Δ::KANMX4 ldb19Δ::NATMX bar1Δ::URA3 FUS1prom-eGFP::LEU2*	This study
BJ5459	*MAT**a** ura3-52 trp1 lys2-801 leu2Δ1 his3Δ200 pep4Δ::HIS3 prb1Δ1.6R can1 GAL cir+*	160
BJ5459 GEV (JT6743)[b]	*MAT**a** ura3-52 trp1 lys2-801 leu2Δ1 his3Δ200 pep4Δ::HIS3 prb1Δ1.6R can1 GAL leu2Δ1::GEV::NATMX*	This study
cnb1Δ	*MAT**a** leu2Δ0 ura3Δ0 his3Δ1 met15Δ0 cnb1Δ::KANMX4*	Yeast deletion collection (Open Biosystems, Inc.)
cna1Δ cna2Δ (JT5574)	*MAT**a** leu2Δ0 ura3Δ0 his3Δ1 met15Δ0 cna1Δ::KANMX4 cna2Δ::KANMX4*	116
JRY11	*MAT**a** ura3-52 trp1 lys2-801 leu2-Δ1 his3-Δ200 pep4Δ::HIS3 prb1-Δ1.6R can1 GAL CNA2-S-TEV-ZZ-KAN^rMX6 CNA1-GFP-LEU2*	116
cnb1Δ GEV (JT6694)[b]	*MAT**a** leu2Δ0 ura3Δ0 his3Δ1 met15Δ0 leu2Δ0::GEV::NATMX cnb1Δ::KANMX4*	This study
cna1Δ cna2Δ GEV (JT6695)[b]	*MAT**a** leu2Δ0 ura3Δ0 his3Δ1 met15Δ0 leu2Δ0::GEV::NATMX cna1Δ::KANMX4 cna1Δ::KANMX4*	This study

[a] To generate strains with the integrated *FUS1prom*-eGFP reporter, the cassette (73) was amplified by PCR and introduced by DNA-mediated transformation into a *bar1Δ* derivative of BY4741. The resulting strain (JT6686) was mated to a *MATα lbd19Δ rod1Δ rog3Δ bar1Δ* mutant. The resulting diploids were sporulated, and *MAT**a** ldb19Δ rod1Δ rog3Δ ldb19Δ bar1Δ FUS1prom*-eGFP spores were identified after tetrad dissection.

[b] To generate a GEV-expressing version of the indicated yeast strain, pACT1-GEV (69, 161) was digested with EcoRV and introduced into the cells of interest by DNA-mediated transformation (65), and nourseothricin (NAT)-resistant colonies were selected in which GEV (expressed under the control of an *ACT1* promoter) is integrated at the *leu2Δ0* locus.

Dura extended-duration substrate (Thermo Scientific, Rockford, IL) detected with Biomax XAR film (Eastman Kodak, Rochester, NY).

Protein purification. GST-Rod1 fusions were used to assess the role of the apparent PXIXIT motif ([545]PQIKIE[550]) in this α-arrestin in mediating its association with calcineurin as follows. Cells of yeast strain JRY11,

which expresses Cna1-GFP, were transformed with pEGKG-Rod1[WT] or pEGKG-Rod1[AQAKAA]. The resulting transformants were grown to mid-exponential phase in SC-2% raffinose, and then expression of the α-arrestin was induced by addition of 2% galactose (final concentration). To activate calcineurin, cells were treated with 200 mM CaCl$_2$ (final concen-

TABLE 2 Plasmids used in this study

Plasmid	Genotype	Description/reference
pEGKG	$GAL1_{prom}$-GST 2μm $URA3$	162
pEGKG-Rod1	$GAL1_{prom}$-GST 2μm $URA3$	163
pEGKG-Rog3	$GAL1_{prom}$-GST 2μm $URA3$	163
pEGKG-Ldb19	$GAL1_{prom}$-GST 2μm $URA3$	163
pEGKG-Art5	$GAL1_{prom}$-GST 2μm $URA3$	163
pEGKG-Rod1^{PANA} (pJT4954)[a]	$GAL1_{prom}$-GST 2μm $URA3$	This study
pEGKG-Rod1^{PASA} (pJT4955)[a]	$GAL1_{prom}$-GST 2μm $URA3$	This study
pEGKG-Rod1$^{PPXY-less}$ (pJT4956)[a]	$GAL1_{prom}$-GST 2μm $URA3$	This study
pEGKG-Rod1^{4KR} (Rod1$^{K235R\ K245R\ K264R\ K267R}$) (pJT5045)[a]	$GAL1_{prom}$-GST 2μm $URA3$	This study
pEGKG-Rog3^{PANA} (pJT4958)[a]	$GAL1_{prom}$-GST 2μm $URA3$	This study
pEGKG-Rog3^{PASA} (pJT4959)[a]	$GAL1_{prom}$-GST 2μm $URA3$	This study
pEGKG-Rog3$^{PPXY-less}$ (pJT4960)[a]	$GAL1_{prom}$-GST 2μm $URA3$	This study
pEGKG-Rog3^{VASA} (pJT4978)[a]	$GAL1_{prom}$-GST 2μm $URA3$	This study
pEGKG-Rog3$^{V/PPXY-less}$ (pJT4979)[a]	$GAL1_{prom}$-GST 2μm $URA3$	This study
pEGKG-Rog3$^{\Delta400}$ (pJT4983)[a]	$GAL1_{prom}$-GST 2μm $URA3$	This study
pEGKG-Rog3^{4KR} (Rog3$^{K235R\ K245R\ K264R\ K267R}$) (pJT5060)[a]	$GAL1_{prom}$-GST 2μm $URA3$	This study
pEGKG-Rod1^{AQAKAA} (pJT4957)[a]	$GAL1_{prom}$-GST 2μm $URA3$	This study
pRS313	$CEN\ HIS3$	164
pRS313-Ldb19 (pJT4963)[b]	$LDB19_{prom}\ CEN\ HIS3$	This study
pRS313-Ldb19^{PAIA} (pJT4964)[c]	$LDB19_{prom}\ CEN\ HIS3$	This study
pRS313-Ldb19^{PPCY} (pJT4965)[c]	$LDB19_{prom}\ CEN\ HIS3$	This study
pRS313-Ldb19$^{PPXY-less}$ (pJT4966)[c]	$LDB19_{prom}\ CEN\ HIS3$	This study
pRS313-Ldb19^{K486R} (pJT5001)[c]	$LDB19_{prom}\ CEN\ HIS3$	This study
pGEX4T1-GST-Ste2$^{297–431}$	$T7\ AMP$	163

[a] Generated by site-directed mutagenesis (67) with synthetic oligonucleotides containing the desired codon alterations (using the wild-type sequence in pRS313 vectors as the template). DNA from the corresponding gene was amplified from genomic DNA by PCR (66) and then cloned into pEGKG.
[b] DNA of the corresponding gene was amplified from genomic DNA by PCR (66) and then cloned into the XmaI-NotI sites in pRS313 (164).
[c] Generated by site-directed mutagenesis with synthetic oligonucleotides containing the desired codon alterations and the corresponding $LDB19$ DNA inserted into pRS313 as the template.

tration) for 10 min and then incubated for 1 h either with vehicle alone (90% [vol/vol] ethanol and 10% [vol/vol] aqueous Tween 20; designated ET) or with the potent and specific calcineurin inhibitor FK506 at a final concentration of 1 μg/ml (added from a 10-mg/ml stock dissolved in ET) prior to galactose induction. After further incubation for 3.5 h, the cells were harvested and lysed by vigorous vortex mixing with glass beads in radioimmunoprecipitation assay (RIPA) buffer (150 mM NaCl, 1 mM EDTA, 1% Triton X-100, 1 mM dithiothreitol [DTT], 50 mM Tris-HCl [pH 7.4]) containing protease inhibitors (77). After brief centrifugation to remove unbroken cells and debris, the clarified extracts were incubated with glutathione-agarose beads (GE Healthcare, Little Chalfont, Buckinghamshire, United Kingdom) for 2 h at 4°C and washed 3 times with 500 μl RIPA buffer. Bound proteins were eluted from the beads in SDS-PAGE sample buffer and resolved by SDS-PAGE, and the presence of Cna1-GFP and GST-Rod1 was analyzed by immunoblotting.

To assess *in vivo* phosphorylation of Rod1, pEGKG-Rod1 and pEGKG-Rod1^{AQAKAA} were introduced into BY4741 and otherwise isogenic $cnb1\Delta$ and $cna1\Delta\ cna2\Delta$ derivatives by DNA-mediated transformation (65). Transformants were grown to mid-exponential phase in SC-2% raffinose. Cells were then treated with either ET alone or 1 μg/ml FK506 in ET for 1 h, and then α-arrestin expression was induced by addition of 4% galactose (final concentration) followed by growth at 30°C for 4 h. Ten minutes prior to harvesting, the cultures were treated with 200 mM CaCl$_2$ (final concentration) to activate calcineurin. Protein extracts were prepared by glass bead lysis in RIPA buffer containing both 600 mM NaCl (HS-RIPA) and 1 μg/ml FK506. After clarification by centrifugation, GST-Rod1 and GST-Rod1^{AQAKAA} were collected from the lysates by binding to glutathione-agarose for 2 h at 4°C. The beads were washed 2 times with 500 μl HS-RIPA, and aliquots of the bead-bound proteins were incubated at 30°C for 45 min either in phosphatase buffer alone (1 mM MnCl$_2$, 10 mM NaCl, 2 mM DTT, 0.01% Brij-35, 50 mM HEPES [pH

7.5]) or in the same buffer containing 200 U of lambda phosphatase (New England BioLabs) in either the absence or presence of phosphatase inhibitors (10 mM Na$_4$P$_2$O$_7$, 10 mM NaF, 0.4 mM NaVO$_3$, 0.4 mM Na$_3$VO$_4$, and 0.1 mM glycerol-3-phosphate). Supernatant liquid was removed by aspiration. Bound protein was eluted at 37°C for 15 min in SDS-PAGE sample buffer, resolved by SDS-PAGE (6% acrylamide gel), and analyzed by immunoblotting.

Assessment of Rsp5 copurification with α-arrestins was performed as described previously (78). To assess the state of α-arrestin modification by ubiquitin *in vivo*, BJ5459 *GEV* cells carrying a plasmid vector (pEGKG) for the expression of GST-Ldb19 or GST-Ldb19(K486R) were grown to midexponential phase and induced with 20 μM β-estradiol (final concentration) for 3 h. After harvesting by centrifugation, the cells were washed and frozen in liquid N$_2$. Cell pellets were resuspended in 600 μl immunoprecipitation buffer (100 mM NaCl, 0.2% Triton X-100, 15 nM EGTA, 50 mM Tris [pH 7.4]) containing 5 mM *N*-ethylmaleimide (NEM) and protease inhibitors (1 tablet of cOmplete protease inhibitor cocktail [Roche Applied Science] per 15 ml) and lysed at 4°C by vigorous vortexing with ~1-g glass beads (0.5 mm; BioSpec Products). After clarification, GST-tagged proteins were recovered from equal volumes of these extracts by incubation with GST-agarose beads for 2 h at 4°C. After two washes with coimmunoprecipitation buffer containing 150 mM NaCl, liquid was removed by aspiration and the beads were resuspended in SDS-PAGE sample buffer to elute the bound proteins, which were resolved by SDS-PAGE and analyzed by immunoblotting.

***In vitro* ubiquitinylation.** The ability of α-arrestins to serve as substrates for Rsp5-mediated ubiquitinylation *in vitro* was assessed by minor modifications of previous methods (79). Briefly, GST-Rsp5 and a catalytically inactive mutant (GST-Rsp5^{C777A}) were expressed in and purified from *Escherichia coli* and the GST tag removed by cleavage with commercial rhinovirus 3C protease (PreScission; GE Healthcare). Uba1 (E1) and

Ubc1 (E2) were purified from yeast as previously described (80). Plasmid DNA (1 µg) of a vector (pME32) carrying the open reading frames for either *ROD1*, *ROG3*, *LDB19*, or cognate derivatives containing mutated versions of one or more of their P/VPXY motifs was used as the template to generate the corresponding [^{35}S]methionine ([^{35}S]Met)-labeled protein by coupled *in vitro* transcription-translation using the TNT quick coupled system (Promega, Sunnyvale, CA). The resulting translation mixture was treated with a final concentration of 10 mM NEM for 15 min at room temperature to inactivate the deubiquitinating enzymes and ubiquitin-conjugating enzymes in the rabbit reticulocyte lysate (81). After quenching unreacted NEM with a final concentration of 20 mM DTT, portions (42 µl) of each *in vitro* translation product were added to a reaction mixture (60 µl final volume) containing the following components at the indicated final concentrations: 600 µM ubiquitin (Sigma, St. Louis, MO), 0.5 mM ATP, 220 nM Uba1, and 3 µM Ubc1. An aliquot (10 µl) was removed as the zero time point, and the reaction was initiated immediately thereafter by addition of GST-Rps5 or, as a control, GST-Rsp5^{C777A} (100 nM final concentration). Additional aliquots were removed at 5, 15, and 30 min, and each was quenched by immediate mixing with 8× concentrated SDS-PAGE sample buffer followed by incubation at 37°C for 15 min. The resulting products were resolved by SDS-PAGE (4.5% acrylamide gel). After drying the gel, the radioactive species were detected by exposure to a phosphorimager screen for 2 h followed by visualization on a Typhoon FLA 7000 laser scanner (GE Healthcare).

Fluorescence microscopy. Imaging of Ste2-mCherry was performed as described previously (21). Imaging of Ste2-GFP was carried out as described previously (82), using an inverted fluorescence microscope (Axiovert 200; Carl Zeiss GmbH, Jena, Germany) equipped with a charge-coupled-device (CCD) camera (Sensicam; PCO-Tech, Inc., Romulus, MI), an X-Cite 120 PC fluorescence illumination system (Exfo Ltd., Quebec, Canada), and a 100× (1.4-numeric-aperture) Plan-Apochromat objective. The day before examining the cells, cultures of the strains to be tested were streaked at a low dilution on plates containing minimal medium (yeast nitrogen base), supplemented with appropriate nutrients to select for plasmid maintenance (if needed), and grown overnight at 30°C, yielding small colonies in mid-exponential-phase growth (as judged by the presence of cells in all cell cycle stages in the population). Single colonies were suspended in 2.75 µl of the same medium on the surface of a glass slide under a coverslip immediately before imaging at room temperature using Slidebook software (v5.0.0.32; Olympus America, San Jose, CA) with identical imaging parameters (2 by 2 binning, 500-ms exposure) for all samples. Images were processed using ImageJ (v1.48b) with identical maximum and minimum intensity values applied to all images.

RESULTS

Ldb19, Rod1, and Rog3 negatively regulate the mating pathway. We first tested whether any of 12 of the 14 recognized yeast α-arrestins affects the function of the Ste2 GPCR. To explore this possibility, we tested derivatives of a *MAT***a** strain (BY4741) harboring an α-arrestin deletion for their response to mating pheromone using a standard agar diffusion bioassay. We did not examine Spo23 (83), which is expressed only in meiotic cells (84), or Bul3, which can be expressed only by translational readthrough of a stop codon situated between two adjacent open reading frames (85). We also tested strains containing deletions of both members of paralogous pairs of α-arrestins or deletions of 9 α-arrestins in combination (*9arr*Δ) (58). A modest but readily detectable and reproducible increase in pheromone sensitivity (as judged by the diameter of the halo of G$_1$-arrested cells) was observed for the *9arr*Δ mutant, an *ldb19*Δ mutant, and a *rod1*Δ *rog3*Δ double mutant (Fig. 1A and B) (however, not *rod1*Δ or *rog3*Δ single mutants [data not shown]). Rod1 and Rog3 share greater similarity to each other (45% identity) than to any other α-arrestin (≤30% identity), suggesting that this pair has an overlapping function. None

of the other single deletions or deletions of any of the other four paralogous pairs, e.g., *aly1*Δ *aly2*Δ (Aly1/Art6 and Aly2/Art3 share 42% identity), exhibited a change in halo size (Fig. 1A, upper, and B). Thus, the effects observed were specific to just three α-arrestins, Ldb19, Rod1, and Rog3.

Neither the *ldb19*Δ mutant nor the *rod1*Δ *rog3*Δ double mutant exhibited the same increase in halo size displayed by the *9arr*Δ cells; however, *ldb19*Δ, *rod1*Δ, and *rog3*Δ are among the deletions carried by the *9arr*Δ cells. Hence, we constructed the corresponding triple mutant, and as anticipated, we found that the pheromone sensitivity of *ldb19*Δ *rod1*Δ *rog3*Δ cells phenocopied that of the *9arr*Δ cells (Fig. 1A, lower, and B). These data suggest that the absence of these three α-arrestins is responsible for the observed behavior of the *9arr*Δ cells. Moreover, despite the fact that these cells possess all of the previously characterized mechanisms for recovery and adaptation, these three α-arrestins clearly contribute to downregulation of pheromone signaling. Furthermore, the fact that the effects of an *ldb19*Δ mutation are additive to those of *rod1*Δ *rog3*Δ provides evidence that Ldb19 acts independently of Rod1 and Rog3.

Ldb19, Rod1, and Rog3 function independently from Bar1 and Sst2. Some α-arrestins have been implicated in aspects of vesicle-mediated transport other than endocytosis (86). Therefore, it was possible that lack of Ldb19, Rod1, and/or Rog3 enhances pheromone response simply by impeding the action of known negative regulators of pheromone signaling that require membrane trafficking (such as the secreted α-factor protease Bar1/SstI) or membrane interaction (such as the receptor- and G-protein-associated RGS protein Sst2). However, compared to an otherwise isogenic *bar1*Δ mutant, an *ldb19*Δ *bar1*Δ double mutant, a *rod1*Δ *rog3*Δ *bar1*Δ triple mutant, and an *ldb19*Δ *rod1*Δ *rog3*Δ *bar1*Δ quadruple mutant exhibited significantly greater pheromone sensitivity at every concentration of α-factor tested (Fig. 1C). Because Bar1 is absent from these cells, the observed additive behavior shows that the increase in pheromone sensitivity has nothing to do with preventing efficient Bar1 secretion or function. Likewise, compared to an otherwise isogenic *sst2*Δ mutant, an *ldb19*Δ *sst2*Δ double mutant, a *rod1*Δ *rog3*Δ *sst2*Δ triple mutant, and an *ldb19*Δ *rod1*Δ *rog3*Δ *sst2*Δ quadruple mutant exhibited greater pheromone sensitivity at every concentration of α-factor tested (Fig. 1D). Again, this additive effect indicates that the absence of Ldb19, Rod1, and/or Rog3 does not cause increased pheromone sensitivity by interfering with Sst2 action. Because these α-arrestins negatively regulate pheromone response by a mechanism(s) independent from those exerted by either Bar1 or Sst2, we used *bar1*Δ and *sst2*Δ cells as sensitized backgrounds in which to further characterize the function of Ldb19, Rod1, and Rog3.

Rod1 and Rog3 promote adaptation. The increased pheromone sensitivity observed when Ldb19 or Rod1 and Rog3 are absent is consistent with a role for these proteins in receptor downregulation and/or signal dampening. If so, overexpression of such negative regulators should stimulate recovery from pheromone signaling. The agar diffusion bioassay provides a convenient means to assess desensitization, because adaptation is readily monitored by examining the rate and extent of the resumption of cell growth inside the initial zone of pheromone-imposed G$_1$ arrest. Normally, in the absence of Sst2, once cells are exposed to pheromone, little or no adaptation is observed even after prolonged incubation (19, 21); only occasional papillae arise (see, for
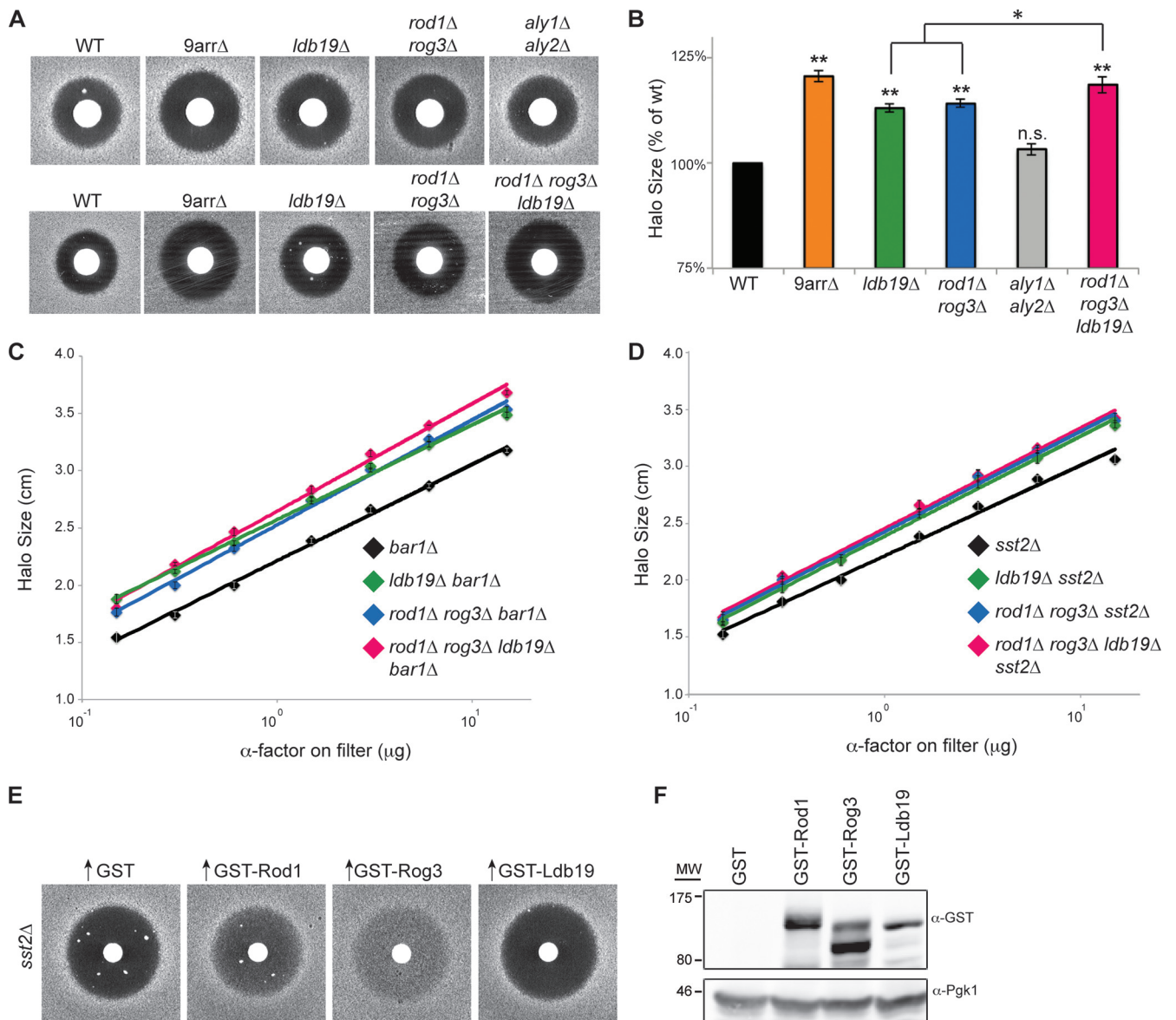
FIG 1 Specific α-arrestins negatively regulate pheromone signaling and act independently from secreted protease Bar1 and RGS protein Sst2. (A) Pheromone sensitivity of wild-type *MAT**a*** cells (BY4741) and otherwise isogenic derivatives containing the indicated α-arrestin deletions (*9arr*Δ, EN60; *ldb19*Δ, BY4741 *ldb19*Δ; *rod1*Δ *rog3*Δ, JT5858; *aly1*Δ *aly2*Δ, D2-6A; *rod1*Δ *rog3*Δ *ldb19*Δ, JT6675) was assessed by the agar diffusion (halo) bioassay for α-factor-induced growth arrest on YPD medium (15 μg α-factor spotted on each filter disk). Data from one representative experiment are shown. (B) Quantification and statistical analysis of the change in halo diameter, determined as described for panel A, for independent replicate experiments ($n = 4$). The average halo diameter for control cells was set at 100%, and halo sizes for each mutant were normalized to the control. Error bars indicate ± standard errors of the means (SEM); **, $P < 0.0001$; *, $P < 0.05$; n.s., value not statistically significant. (C) Pheromone sensitivity of a *MAT**a*** *bar1*Δ strain (JT5915) and otherwise isogenic *ldb19*Δ *bar1*Δ (JT5916), *rod1*Δ *rog3*Δ *bar1*Δ (JT5917), and *rod1*Δ *rog3*Δ *ldb19*Δ *bar1*Δ (JT6674) derivatives was determined as described for panel A in response to the indicated amounts of α-factor (150 ng to 15 μg). Values represent the averages from independent replicate experiments ($n = 5$); errors bars indicate ±SEM. (D) Pheromone sensitivity of a *MAT**a*** *sst2*Δ (JT6755) strain and otherwise isogenic *ldb19*Δ *sst2*Δ (JT6660), *rod1*Δ *rog3*Δ *sst2*Δ (JT6702), and *rod1*Δ *rog3*Δ *ldb19*Δ *sst2*Δ (JT6662) derivatives was determined in response to the indicated amounts of α-factor. Values represent the averages from independent replicate experiments ($n = 3$); errors bars indicate ±SEM. (E) Pheromone sensitivity of a *MAT**a*** *sst2*Δ strain (JT5919) carrying the GEV chimera for β-estradiol-induced expression of genes under *GAL* promoter control and containing either empty vector (high-copy-number *URA3*-marked 2μm DNA plasmid) or the same vector harboring the indicated α-arrestin (as a fusion to GST) under *GAL* promoter control was determined on SC-Ura, as described for panel A, using 15 μg of α-factor spotted on the filter disk after induction with β-estradiol (see Materials and Methods). Data from one representative experiment ($n = 5$) are shown. (F) Confirmation of α-arrestin expression. Proteins from whole-cell extracts of the cells shown in panel E were prepared, resolved by SDS-PAGE, and analyzed by immunoblotting with the indicated antibodies. Data from one representative experiment ($n = 5$) are shown. MW, molecular weight in thousands.

example, Fig. 1E, left), which represent rare cells with a selective advantage (they became pheromone resistant by acquiring a spontaneous *ste* mutation) (87). Remarkably, overexpression of either GST-Rod1 or GST-Rog3 in *sst2*Δ cells caused turbid halos diag-

nostic of adaptation, recovery from G₁ arrest, and a return to cell growth (Fig. 1E). Similar turbid halos have been observed when other negative regulators of pheromone response are overexpressed (88). Although both α-arrestins are produced at an equiv-

alent level (Fig. 1F), the adaptation-promoting effect of GST-Rog3 was reproducibly more potent than that of GST-Rod1.

In contrast, overexpression of GST-Ldb19, or untagged Ldb19 (data not shown), in $sst2\Delta$ cells did not promote adaptation (Fig. 1E). In multiple trials, GST-Ldb19 expression was always lower than that of GST-Rod1 and GST-Rog3 (Fig. 1F). Therefore, it was formally possible that the level of GST-Ldb19 achieved was insufficient to support adaptation. However, like GST-Ldb19, other GST-tagged α-arrestins that are expressed at a level comparable to or even higher than that of GST-Rod1 and GST-Rog3 (e.g., GST-Art5 and GST-Csr2/Art8) also failed to promote adaptation in $sst2\Delta$ cells (data not shown). These observations argue, first, that the adaptation-promoting effects of Rod1 and Rog3 are specific. Second, and tellingly, because α-factor is present continuously in these assays, these observations indicate that Rod1 and Rog3 act on the pheromone receptor in its ligand-occupied conformation, whereas Ldb19 is unable to do so. These data also show that Rod1 and Rog3 act at a different level and/or via a different mechanism than Ldb19. Of course, some other factor may be rate limiting for the Ldb19-promoted adaptation pathway (such as a stimulus that results in more receptor misfolding or unfolding [see Discussion]).

Absence of α-arrestins and mating pathway signaling. Pheromone-imposed G_1 arrest is one measure of mating pathway function. We used two other independent methods to confirm that absence of α-arrestins leads to an enhanced pheromone response. First, under conditions where the concentration of α-factor remains essentially constant (cells carried a $bar1\Delta$ mutation), we compared the kinetics of activation (via dual phosphorylation) of Fus3 (89), the mating pheromone response pathway-specific MAPK (12, 90), after exposing an otherwise wild-type strain and an $ldb19\Delta$ $rod1\Delta$ $rog3\Delta$ triple mutant to α-factor (Fig. 2A). As observed in the halo bioassay, there was more efficacious and sustained signaling in cells lacking the three α-arrestins than in the control cells, although the effect was relatively modest. $FUS3$ itself is known to be a pheromone-induced gene product (27, 89, 91), and the level of Fus3 increased in control cells and cells lacking Ldb19, Rod1, and Rog3. However, the fraction of Fus3 in its activated state was higher and more persistent in the cells lacking the three α-arrestins than in the control cells (Fig. 2B).

Another standard used to measure pheromone response is induction of the pheromone-responsive gene $FUS1$ (92). We quantified the expression level of an integrated $FUS1_{prom}$-eGFP reporter gene (73) in $bar1\Delta$ cells that were otherwise wild type or carried the $ldb19\Delta$ $rod1\Delta$ $rog3\Delta$ mutations using flow cytometry. It was shown previously that basal signaling in the mating pheromone response pathway arises largely from stochastic spontaneous dissociation of receptor-heterotrimeric G protein complexes (93, 94). An increase in receptor level in the PM shifts the equilibrium toward complex formation and reduces basal signaling (21, 23). For this reason, if the α-arrestin-deficient cells internalize Ste2 less efficiently, then basal signaling should be reduced. Consistent with this prediction, basal expression was significantly lower in cells lacking Ldb19, Rod1, and Rog3 than in control cells (Fig. 2C). Nonetheless, after exposure to α-factor, the level of $FUS1$ expression achieved in the α-arrestin-deficient cells was nearly equivalent to that in the wild type. Therefore, the induction ratio for the $FUS1$ reporter was ~3-fold higher in the $ldb19\Delta$ $rod1\Delta$ $rog3\Delta$ $bar1\Delta$ cells than in $bar1\Delta$ cells (Fig. 2D). Thus, as judged by three different assays, pheromone signaling is more

sustained in cells lacking Ldb19, Rod1, and Rog3 than in control cells, consistent with loss of negative regulation of the pathway.

Efficient Ste2 internalization requires Ldb19, Rod1, and Rog3. In *S. cerevisiae*, various classes of integral polytopic PM proteins can be endocytosed by clathrin-dependent (95) and clathrin-independent (96) routes. Caveolin-like structures in yeast ("eisosomes") (97, 98) do not appear to be sites of endocytosis (99, 100) and may even protect cargo from internalization (101). The evidence that various yeast α-arrestins are necessary for efficient internalization of distinct PM-localized nutrient permeases is compelling (57–59, 102). If Ldb19, Rod1, and/or Rog3 contributes to GPCR downregulation by any endocytic route, one would expect to detect some Ste2 accumulation at the PM in cells lacking one or more of these α-arrestins. To examine receptor localization, we first used full-length Ste2 tagged at its C terminus with mCherry (21). We showed before that in otherwise wild-type cells (even in the absence of pheromone), the red fluorescence resides mainly in the vacuole (21), presumably because maturation of the mCherry chromophore is slow relative to the rate of constitutive endocytosis and/or because the mCherry portion of the fusion persists due to its slow degradation. Indeed, in wild-type cells, the fluorescent signal was confined almost exclusively to the vacuole (Fig. 3A, left), whereas in isogenic $ldb19\Delta$ single, $rod1\Delta$ $rog3\Delta$ double, and $ldb19\Delta$ $rod1\Delta$ $rog3\Delta$ triple mutants, fluorescence was discernible at the PM (Fig. 3A).

To confirm that these conclusions were not dependent on the chromophore used to monitor Ste2 localization and to quantify the results, the same analysis was carried out using cells expressing full-length Ste2 tagged at its C terminus with eGFP. Again, the fluorescent signal in the parental strain was confined largely to the vacuole in virtually every cell, whereas the vast majority of the $9arr\Delta$, $ldb19\Delta$, $rod1\Delta$ $rog3\Delta$, and especially $ldb19\Delta$ $rod1\Delta$ $rog3\Delta$ cells exhibited readily detectable PM fluorescence (Fig. 3B). In marked contrast, the level of Ste2-GFP fluorescence at the PM was unchanged in mutants lacking other α-arrestins, e.g., $aly1\Delta$ $aly2\Delta$ (Fig. 3B). These visual impressions were corroborated by averaging the intensity of PM fluorescence determined by taking multiple line scans across large numbers of cells in each field (Fig. 3C). Together, these results are consistent with Ldb19, Rod1, and Rog3 acting as negative regulators of pheromone-initiated signaling by promoting efficient Ste2 internalization.

The ubiquitin ligase Rsp5 is required for Ldb19 and Rod1 action. Aside from an N-terminal arrestin fold that mediates interaction with specific targets, a defining hallmark of an α-arrestin is that its C-terminal sequence contains multiple copies of PPXY (and/or variants thereof, such as LPXY and VPXY) (Fig. 4A). The PPXY motifs serve as docking sites for binding three tandem WW domains (103) present in the HECT family ubiquitin ligase (E3) Rsp5 (104, 105). In this way, α-arrestins act as adaptors that link PM substrates that lack endogenous PPXY motifs to Rsp5 (106, 107), which catalyzes substrate ubiquitinylation, thereby marking cargo for endocytosis (57, 58, 102, 108). The primary structure of Ste2 has no PPXY motif or variant thereof in its cytoplasmic loops or cytosolic tail, yet it becomes ubiquitinylated in an Rsp5-dependent manner on seven Lys residues in its C-terminal tail (21, 41, 55).

To determine whether Rsp5 recruitment is required for negative regulation of pheromone signaling by Ldb19, Rod1, or Rog3, we first mutated the two PPXY motifs in each of these α-arrestins to PAXA and then used two different methods to assess whether
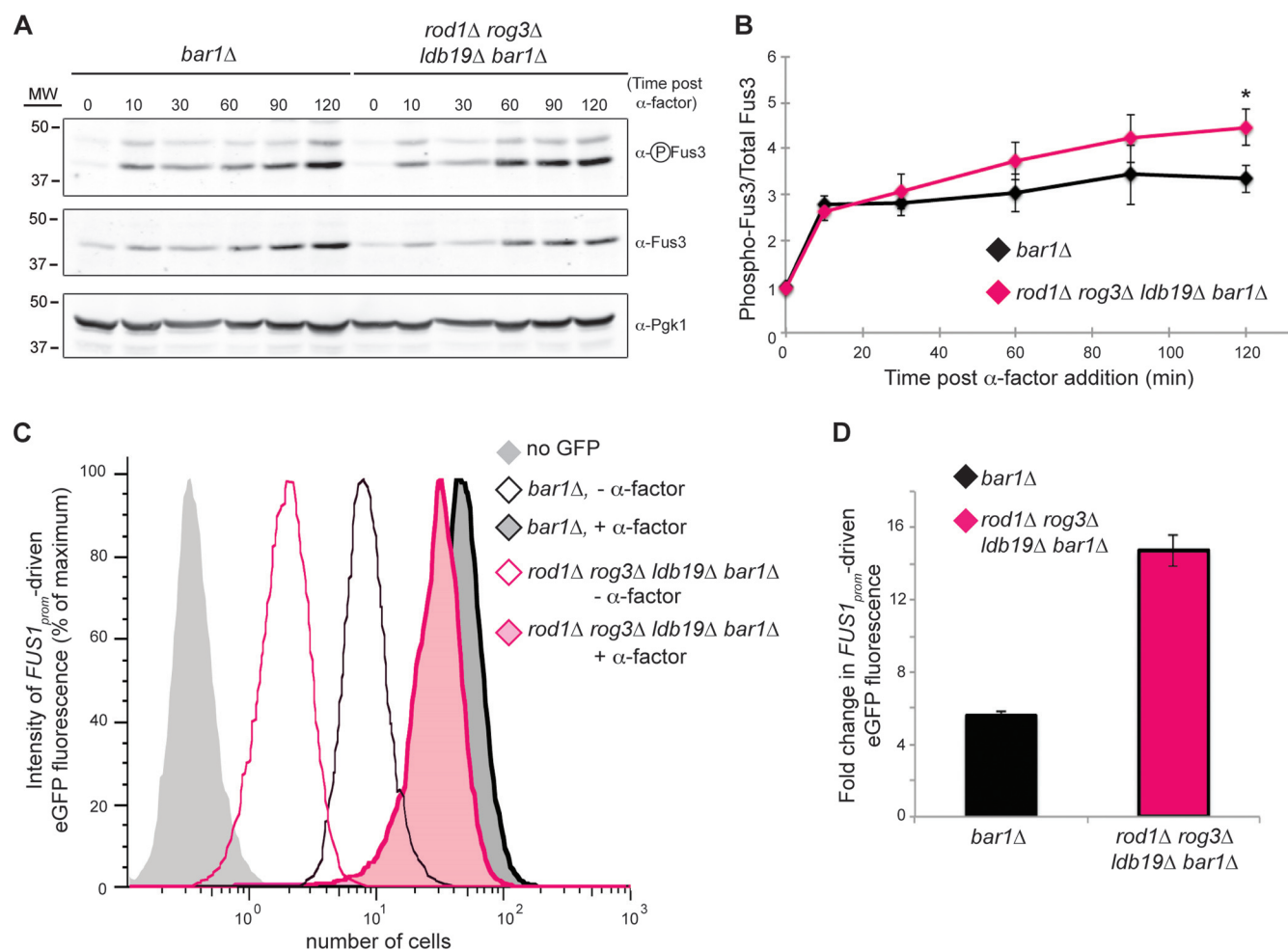
FIG 2 Pheromone signaling is more persistent in cells lacking Ldb19, Rod1, and Rog3. (A) Cultures of a *MAT**a** bar1Δ* strain (JT5915) and an otherwise isogenic *ldb19Δ rod1Δ rog3Δ bar1Δ* derivative (JT6674) were grown to mid-exponential phase and then treated with 15 nM α-factor for the indicated times. Samples were withdrawn at the indicated time points and rapidly chilled on ice. The cells were collected by centrifugation and extracted, and proteins in the resulting whole-cell lysates were resolved by SDS-PAGE and analyzed by immunoblotting with the indicated antibodies. Data from one representative experiment (*n* = 3) are shown. MW, molecular weight in thousands. (B) Values represent the mean pixel intensities for the phosphorylated and total Fus3 bands, determined as described for panel A, from the three independent replicate experiments. Error bars indicate ±SEM; *, *P* < 0.01. (C) Cultures of a *MAT**a** bar1Δ FUS1_prom*-eGFP strain (JT6686) and an otherwise isogenic *ldb19Δ rod1Δ rog3Δ bar1Δ FUS1_prom*-eGFP derivative (JT6668) were grown to mid-exponential phase. Samples of these cultures were withdrawn, and the distribution of fluorescent cells was determined using a fluorescence-activated cell sorter (model FC500; Beckman-Coulter) at the Flow Cytometry Facility of the UC Berkeley Cancer Research Laboratory. The remainder of each culture was treated with 15 nM α-factor for 2 h, and the profile of fluorescent cells in each culture was redetermined. (D) The average fold change in the level of GFP fluorescence determined from the ratio of the areas under the curves of uninduced and pheromone-induced cells of the indicated genotypes for independent replicate experiments (*n* = 3) performed as described for panel C. Error bars indicate ±SEM.

these point mutations successfully abrogated interaction with Rsp5. In the case of Rog3, we also mutated its VPXY motif because an identical motif in α-arrestin Rim8/Art9 was shown to mediate Rsp5 association (109). As observed for other α-arrestins (57, 78, 108), we found that Rsp5 efficiently copurified with GST-Ldb19, GST-Rod1, and GST-Rog3 (and not with a GST control), whereas the corresponding PPXY-less (or, in the case of Rog3, P/VPXY-less) mutants exhibited dramatic decreases in the amount of Rsp5 recovered: Ldb19, 93% reduction; Rod1, 71% reduction; and Rog3, 83% reduction (Fig. 4B). The residual amount of Rsp5 observed for the mutants does not represent residual interaction but rather nonspecific background, because no further reduction below this threshold was observed when a complete C-terminal truncation [Rog3(Δ400-733)] was examined (Fig. 4B). As an independent and more sensitive indicator of the ablation of Rsp5

interaction by these point mutations, we took advantage of the fact that this E3 efficiently ubiquitinylates endogenous Lys residues in the α-arrestins (57, 58, 102, 108). We found that each of the three α-arrestins, prepared by coupled *in vitro* transcription and translation, served as an efficient substrate for Rsp5-dependent ubiquitinylation, as judged by complete conversion of the starting material to a broad spectrum of polyubiquitinylated, slower-mobility species (Fig. 4C). In control reactions incubated with Rsp5^C777A, no detectable ubiquitinylated species were observed (data not shown). As expected, the PPXY point mutations abolished Rsp5-dependent modification of each α-arrestin almost entirely (Fig. 4C). Thus, as judged by two different criteria, the point mutants we generated in Ldb19, Rod1, and Rog3 clearly compromise their interaction with Rsp5.
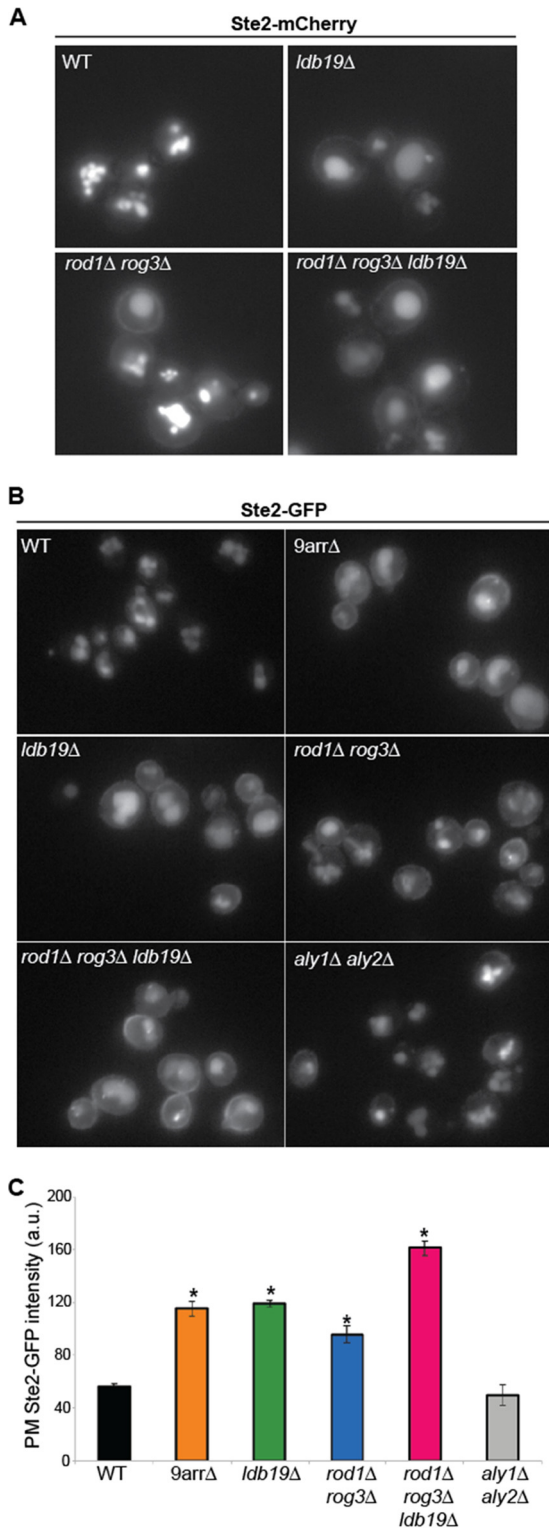
We then used a complementation test to determine if Rsp5

FIG 3 Increased abundance of Ste2 in the plasma membrane in cells lacking Ldb19 and/or Rod1 and Rog3. (A) A *MAT***a** strain expressing an integrated copy of Ste2-mCherry (as the sole copy of this receptor) from the native *STE2* promoter at the endogenous *STE2* locus on chromosome VI (JT6677) and otherwise isogenic *ldb19Δ* (JT6678), *rod1Δ rog3Δ* (JT6679), and *rod1Δ rog3Δ ldb19Δ* (JT6680) derivatives were examined by fluorescence microscopy. Representative images were recorded as described in Materials and Methods. (B) The same as panel A, except the cells expressed an integrated copy of Ste2-GFP

association is required for Ldb19 function in pheromone signal dampening. As described earlier (Fig. 1A), *ldb19Δ bar1Δ* cells display a halo of pheromone-induced growth inhibition that is larger than that of isogenic *bar1Δ* cells (Fig. 5A). Reintroduction of wild-type *LDB19* (expressed from its native promoter on a low-copy-number *CEN* plasmid) into the *ldb19Δ bar1Δ* strain reduced the halo size to that observed in the *bar1Δ* strain, whereas even single PAXA point mutations and the double (PPXY-less) mutant were unable to do so (Fig. 5A and B). Thus, the ability of Ldb19 to down-modulate signaling requires its interaction with Rsp5.

To determine if Rsp5 association is required for either Rod1 or Rog3 function in signal dampening, we exploited their ability to promote recovery and adaptation in *sst2Δ* cells exposed to pheromone, as described earlier (Fig. 1E). Overexpression of wild-type *ROD1* (as a GST fusion from the *GAL1* promoter on a high-copy-number 2μm DNA plasmid) in *sst2Δ* cells produced a turbid halo and reduced halo size, whereas even single PAXA point mutations and the double (PPXY-less) mutant were unable to do so (Fig. 5C, top), even though the Rod1 mutants were expressed at a level as high as or higher than that of the wild-type protein (Fig. 5D). Thus, as for Ldb19, the ability of Rod1 to downregulate signaling also requires its interaction with Rsp5.

Strikingly, as judged by the same assay, overexpression in *sst2Δ* cells of wild-type Rog3, single PAXA mutants, and the double PPXY-less mutant (Fig. 5C, lower), and even the P/VPXY-less derivative lacking all three of its Rsp5-binding motifs (Fig. 5E) produced turbid halos, even though the P/VPXY mutations eliminated the ability of Rog3 to associate with (Fig. 4B) and be modified (Fig. 4C) by Rsp5. Hence, in contrast to Ldb19 and Rod1, the ability of Rog3 to squelch pheromone signaling does not obligatorily require association with Rsp5. However, it was possible that Rog3 associates with its closest paralog, Rod1, to form a heterodimer (or higher oligomer), and Rsp5 recruited by this partner overcomes the loss of the P/VPXY motifs in Rog3. However, this possibility was eliminated (as well as effects of Rog3 mediated through Ldb19) because overexpressed Rog3 and its PPXY-less derivative still promoted efficient adaptation in cells lacking endogenous Ldb19, Rod1, and Rog3 (Fig. 5E). Thus, negative regulation of pheromone signaling by Rog3 does not require interaction, either direct or indirect, with Rsp5. Indeed, just the arrestin fold domain at the N terminus of Rog3 is sufficient to promote desensitization, because overexpression of a truncation mutant, Rog3(Δ400-733), yielded halos just as turbid, if not more so, than those of full-length Rog3. In contrast, Ldb19(Δ447-818) and Rod1(402-837) were nonfunctional (data not shown). Therefore, Rog3 can act on the receptor to negatively regulate signaling by a mechanism that is independent of the other two α-arrestins and Rsp5.

Ubiquitinylation of Ldb19, Rod1, and Rog3 is dispensable for signal dampening. It has been demonstrated that the cognate α-arrestin itself becomes ubiquitinylated during the process of recruiting Rsp5 to nutrient permeases (57, 58, 78, 102, 108). Moreover, the Lys residues in Ldb19 and Rod1 that are ubiquiti-

as the sole source of the receptor, and *9arrΔ* (JT6757) and *aly1Δ aly2Δ* (JT6762) derivatives were also visualized. (C) Mean intensity of PM fluorescence was quantified for each of the indicated strains (≥50 cells each) using ImageJ and plotted in arbitrary units (a.u.). Values significantly different from those of the control cells were assessed using a one-way analysis of variance test with Tukey's *post hoc* comparison (165). *, $P < 0.0001$.
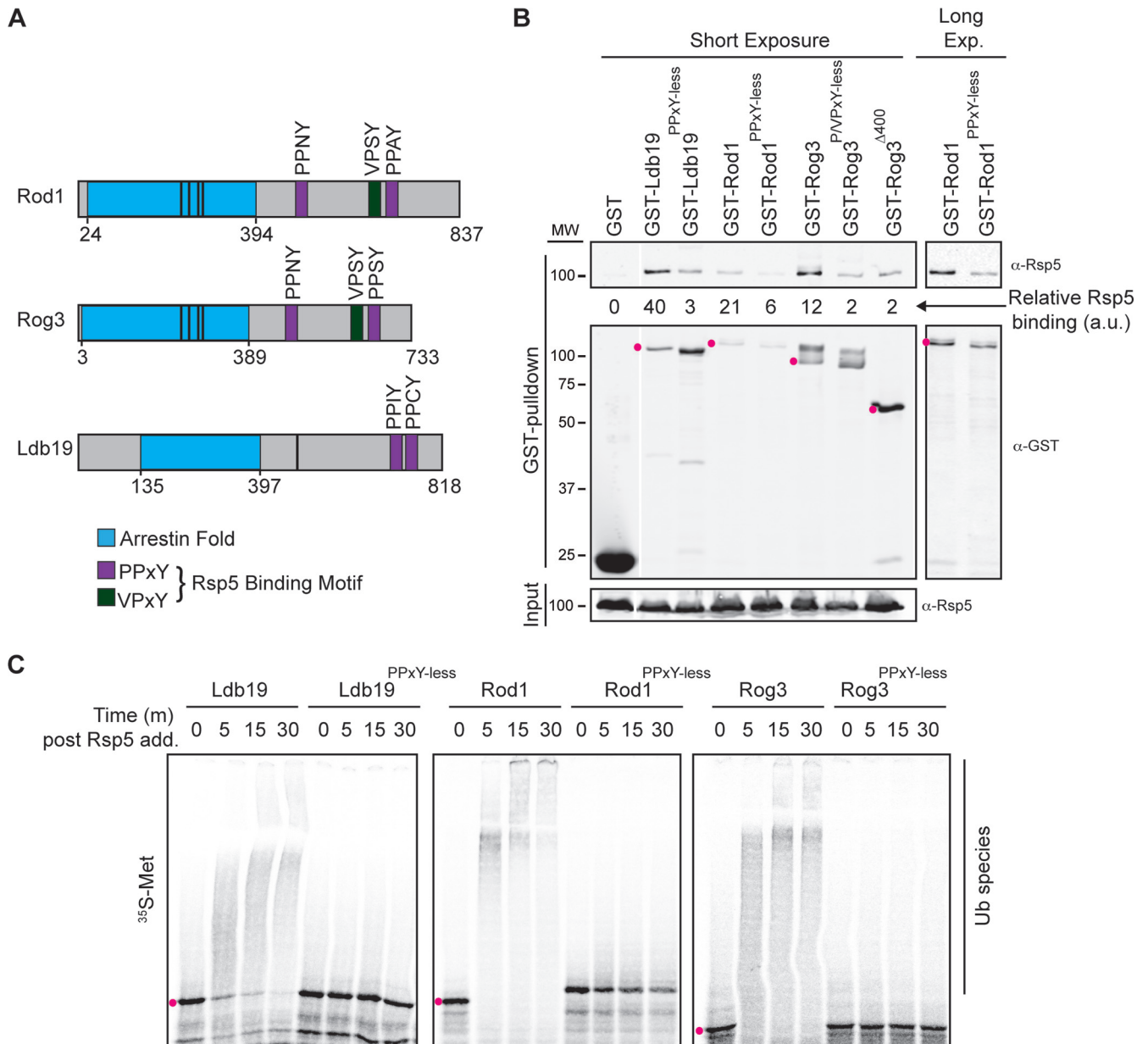
FIG 4 P/VPXY motifs in Ldb19, Rod1, and Rog3 are required for Rsp5 binding and Rsp5-mediated ubiquitinylation. (A) Schematic depiction of the primary structures of Ldb19, Rod1, and Rog3. Residues (numbers below each bar) comprising the arrestin fold (blue) in Ldb19 according to reference 57 and in Rod1 and Rog3 as predicted by the Phyre2 modeling algorithm (166) are shown, and positions of the consensus Rsp5-binding motifs, PPXY and VPXY, and reported ubiquitinylated Lys residue(s) (black lines) are indicated. (B) Cultures of a GEV derivative of vacuolar protease-deficient strain BJ5459 (160) expressing the indicated α-arrestin or the derived P/VPXY substitution mutant (as a GST fusion from the *GAL* promoter) were grown to mid-exponential phase. Protein expression was induced with β-estradiol, and the cells were harvested by centrifugation and ruptured by vigorous vortex mixing with glass beads. GST fusions in the resulting extracts (pink dots) were captured by binding to glutathione-agarose beads. After washing, the bound proteins were resolved by SDS-PAGE and analyzed by immunoblotting with the indicated antibodies. MW, molecular weight in thousands; Long Exp., long exposure. (C) The Rsp5-catalyzed and time-dependent ubiquitinylation of an [^{35}S]Met-labeled α-arrestin or its cognate PPXY substitution mutant (pink dots), prepared by coupled *in vitro* transcription-translation, was performed and analyzed using a phosphorimager as described in Materials and Methods. add., addition; Ub, ubiquitinylation.

nylated have been mapped (Fig. 4A), and it was reported that corresponding K-to-R mutations in Ldb19 and Rod1 block endocytosis of their target nutrient permeases, the arginine transporter Can1 (57) and the lactate transporter Jen1 (102), respectively, suggesting that ubiquitinylation is required for the endocytosis-promoting function of these and other α-arrestins (108).

Our PPXY mutants of Ldb19, Rod1, and Rog3 should prevent

ubiquitinylation of both the α-arrestin and its cargo, because they cannot bind Rsp5. Hence, the failure of PPXY-less versions of Ldb19 (Fig. 5A) and Rod1 (Fig. 5C) to promote signal dampening could be due to defective ubiquitinylation rather than an inability to deliver Rsp5 to the receptor (and/or other targets). To distinguish between these possibilities, we generated K-to-R mutations in the ubiquitinylated sites in Ldb19 (56) and Rod1 (64) to selec-
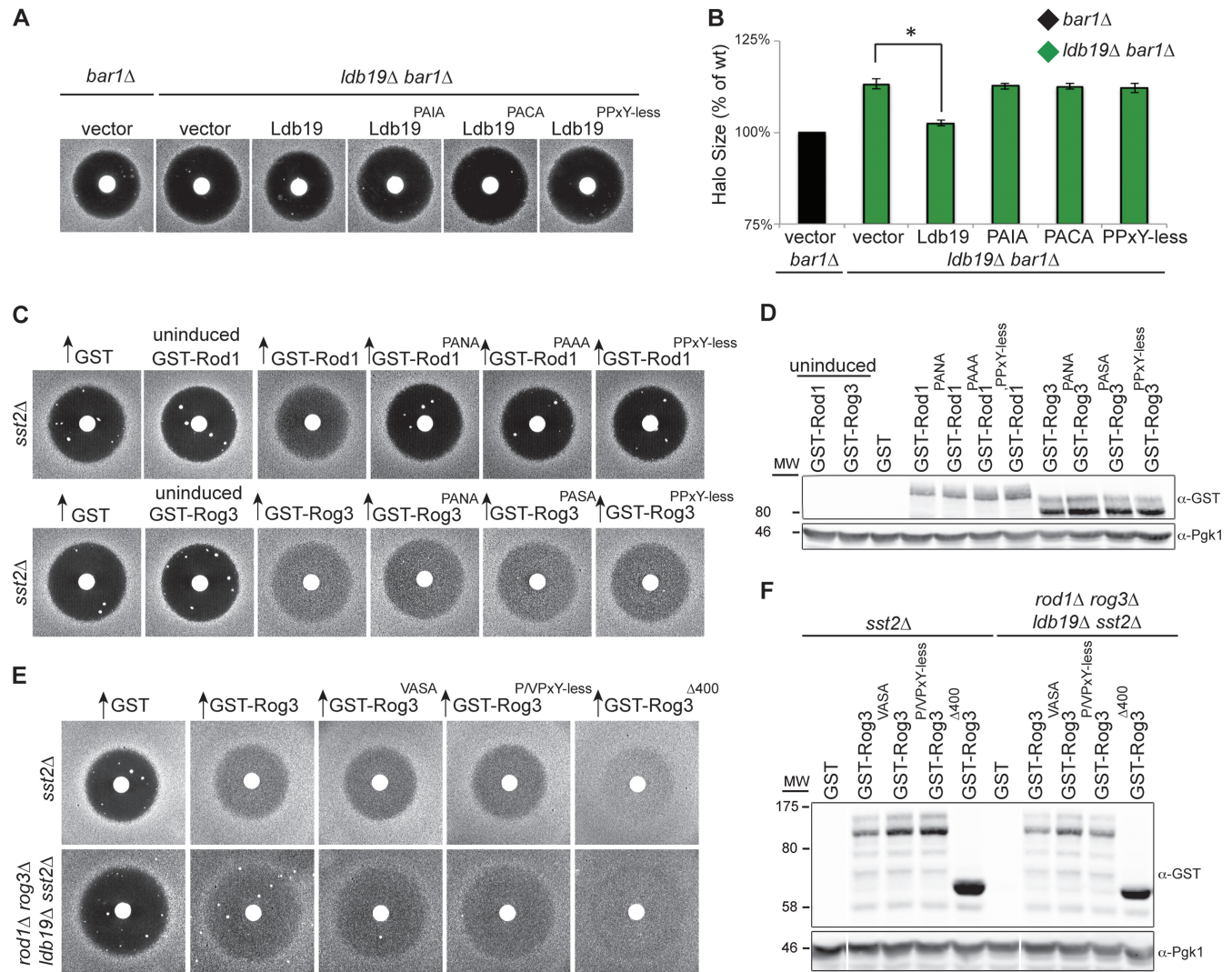
FIG 5 Ldb19 and Rod1, but not Rog3, require Rsp5 binding to downregulate pheromone signaling. (A) Pheromone sensitivity of a *MAT***a** *bar1Δ* strain (JT5915) and an otherwise isogenic *ldb19Δ bar1Δ* derivative (JT5916) carrying either empty vector (*HIS3*-marked *CEN* plasmid) or the same vector expressing wild-type *LDB19* or derivatives containing point mutations in each or both of its PPXY motifs binding was determined as described for Fig. 1A, except that the medium was SC-His. (B) Quantification and statistical analysis of the change in halo diameter, determined as described for panel A, for independent replicate experiments (*n* = 3). The average halo diameter for control cells was set at 100%, and the halo sizes for each mutant were normalized to that of the control. Error bars indicate ±SEM; *, *P* < 0.0001. (C) Pheromone sensitivity of cultures of *MAT***a** *sst2Δ GEV* cells (JT5919) overexpressing either Rod1 or Rog3, as indicated, or the derived PPXY point mutants under the control of the *GAL* promoter on a high-copy-number *URA3*-marked 2μm DNA plasmid was determined as described in the legend to Fig. 1E. Data from one representative experiment (*n* = 5) are shown. (D) Proteins from whole-cell extracts of the cells shown in panel C were prepared, resolved by SDS-PAGE, and analyzed by immunoblotting with the indicated antibodies. Data from one representative experiment (*n* = 5) are shown. MW, molecular weight in thousands. (E) Pheromone sensitivity of cultures of *MAT***a** *sst2Δ GEV* cells (JT5919) or an *ldb19Δ rod1Δ rog3Δ sst2Δ GEV* derivative (JT6716) overexpressing either Rog3 or the derived cognate P/VPXY point mutants, under the control of the *GAL* promoter on a high-copy-number *URA3*-marked 2μm DNA plasmid, was determined as described for panel C. Data from one representative experiment (*n* = 3) are shown. (F) Confirmation of protein expression, as described for panel D. Data from one representative experiment (*n* = 3) are shown.

tively disrupt their ubiquitinylation but leave Rsp5 binding intact. First, we generated GST-Ldb19(K486R) (57) and confirmed by pulldown, SDS-PAGE analysis, and immunoblotting that GST-Ldb19 is ubiquitinylated *in vivo*, whereas GST-Ldb19(K486R) is not (Fig. 6A, upper). Strikingly, as judged by the complementation test, reintroduction of either wild-type *LDB19* or *LDB19(K486R)* into the *ldb19Δ bar1Δ* strain reduced the halo size to that observed in the *bar1Δ* strain (Fig. 6B and C). Thus, the ability of Ldb19 to down-modulate signaling requires Rsp5 interaction (Fig. 5A) but does not require its own ubiquitinylation.

We next generated GST-Rod1(K235R K245R K264R K267R),

here termed Rod1[4KR], based on published data about the ubiquitinylation sites in Rod1 (102), and confirmed that the 4K-to-R mutations abrogate its ubiquitinylation *in vivo* (Fig. 6A, lower). As assessed by the adaptation assay, overexpression of either wild-type *ROD1* or *ROD1[4KR]* in *sst2Δ* cells produced equally turbid halos (Fig. 6D). Hence, the ability of Rod1 to downregulate signaling also requires Rsp5 interaction (Fig. 5C) but apparently not its own ubiquitinylation.

The Lys residues we mutated in Rod1 are conserved at the equivalent positions in Rog3; hence, we generated GST-Rog3(K235R K245R K264R K267R), here termed Rog3[4KR]. In the
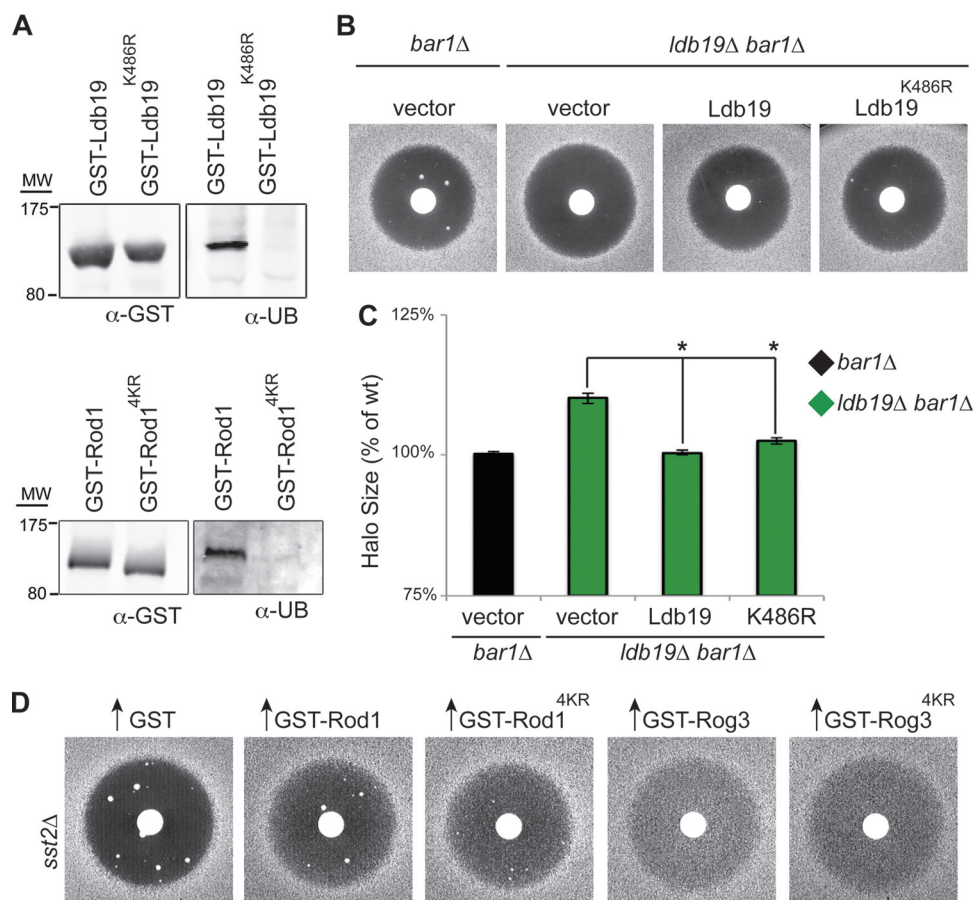
FIG 6 Ubiquitinylation of Ldb19, Rod1, and Rog3 is not required for downregulation of pheromone signaling. (A) For analysis of *in vivo* ubiquitinylation of Ldb19, cultures of a GEV derivative of BJ5459 (JT6743) were grown to mid-exponential phase. Expression of either Ldb19 or the derived K486R substitution mutant (as a GST fusion from the *GAL* promoter) was then induced with β-estradiol for 3 h, and lysates were immediately prepared and analyzed as described for Fig. 4B using the indicated antibodies. For analysis of *in vivo* ubiquitinylation of Rod1, cells were grown to mid-exponential phase in 4% raffinose. Expression of either Rod1 or the derived 4K-to-R mutant (as a GST fusion from the *GAL* promoter) was induced by addition of galactose (2% final concentration) for 3 h and then shifted to dextrose medium (2% final concentration) for 5 min, and lysates were immediately prepared and analyzed as described for Fig. 4B. MW, molecular weight in thousands. (B) Pheromone sensitivity of a *MAT*a *bar1*Δ (JT5915) strain and an isogenic *ldb19*Δ *bar1*Δ derivative (JT5916) carrying either empty vector (*HIS3*-marked *CEN* plasmid) or the same vector expressing wild-type *LDB19* or the K486R substitution mutant was determined as described in the legend to Fig. 1A, except that the medium was SC-His. (C) Quantification and statistical analysis of the change in halo diameter, determined as described for panel B, from independent replicate experiments (*n* = 3). The average halo diameter for control cells was set at 100%, and the halo sizes for each mutant were normalized to the control. Error bars indicate ±SEM; *, *P* < 0.0001. (D) Pheromone sensitivity of cultures of *MAT*a *sst2*Δ *GEV* cells (JT5919) expressing either GST-Rod1 or GST-Rog3, as indicated, or the derived 4K-to-R substitution mutants under the *GAL* promoter on a high-copy-number *URA3*-marked 2μm DNA plasmid was determined as described for Fig. 1E. Data from one representative experiment (*n* = 3) are shown.

adaptation assay, overexpression of either wild-type *ROG3* or *ROG3*[4KR] in *sst2*Δ cells produced turbid halos (Fig. 5D). Thus, the ability of Rog3 to squelch signaling requires neither its Rsp5 interaction (Fig. 5C and E) nor, presumably, its own ubiquitinylation (assuming that, as in Rod1, the 4K-to-R mutations eliminate Rog3 ubiquitinylation).

Ldb19, Rod1, and Rog3 associate with the C-terminal cytosolic tail of Ste2. Extraction of the receptor from membranes requires addition of detergent (21, 110), which might cause misfolding and disrupt protein-protein interactions. Cumulative evidence indicates that one of the most dramatic changes that occurs in the receptor upon pheromone binding *in situ* is a conformational alteration that makes its C-terminal extension (cytosolic tail) more susceptible to attack by exogenously added trypsin (111), to greatly enhanced Yck1- and Yck2-dependent phosphorylation (21, 37, 38, 41), and to overt Rsp5-dependent ubiquitiny-

lation at multiple sites (41, 55). These findings suggest that Ldb19, Rod1, and/or Rog3 interact with this same region of the receptor once it becomes exposed, facilitating Rsp5-dependent modification. Hence, we examined the ability of these α-arrestins to interact with a purified soluble version of the 135-residue C-terminal extension of Ste2 [GST-Ste2(297-431)] bound to beads. Moreover, because we demonstrated (Fig. 6) that ubiquitinylation of Ldb19, Rod1, and Rog3 is not required for their actions *in vivo*, it was not necessary to prepare ubiquitin-decorated versions of each molecule to analyze their ability to associate with the Ste2 tail *in vitro*. Indeed, we found that ^{35}S-labeled Ldb19, Rod1, and Rog3 reproducibly bound better to the C-terminal tail of Ste2 than to the GST control (Fig. 7A and B). Other α-arrestins (e.g., Aly1/Art6) and Art5 (data not shown) did not show any increase above the level of the control (Fig. 7A and B). Moreover, consistent with the fact that its overexpression promoted recovery of *sst2*Δ cells,
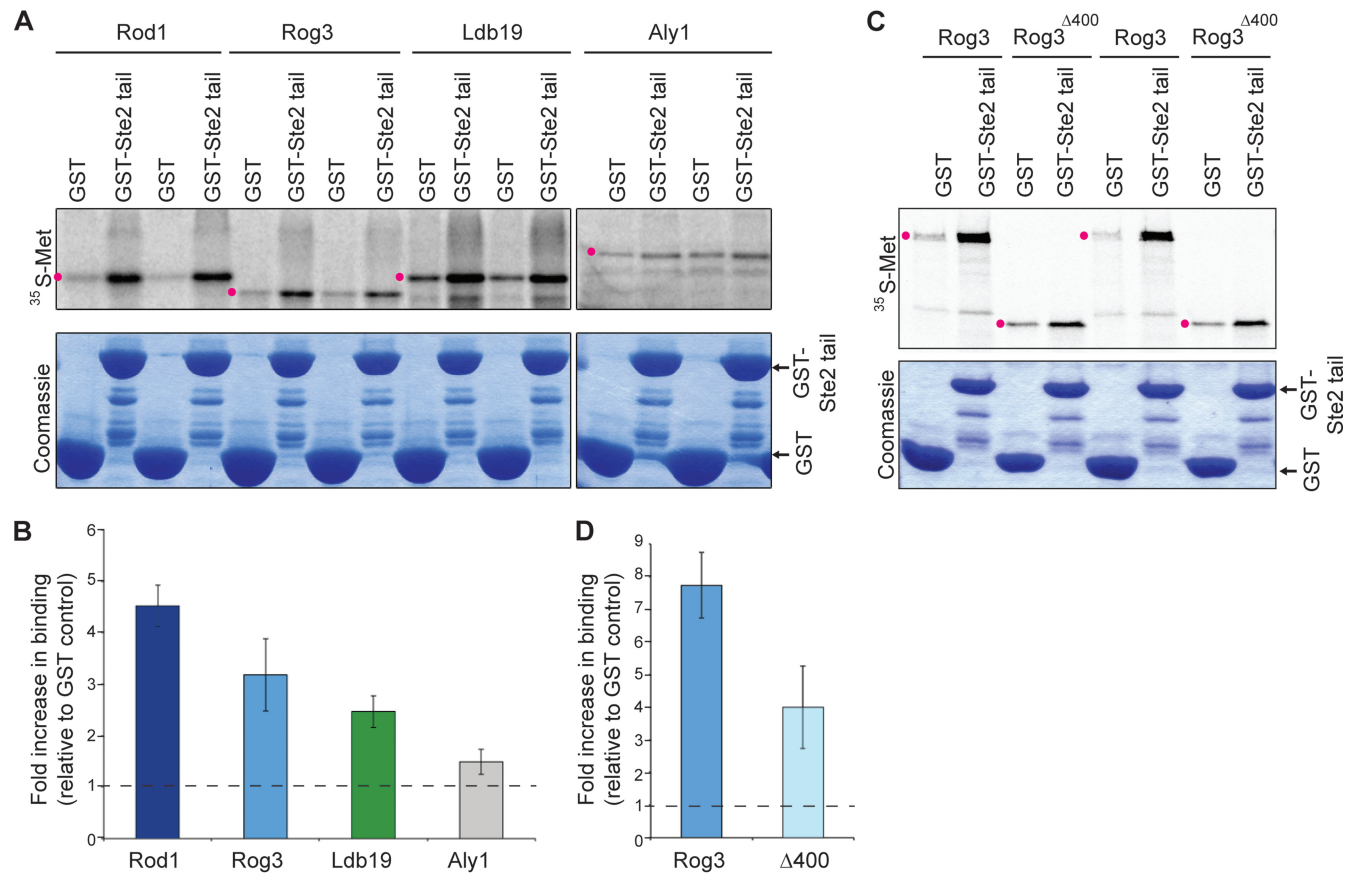
FIG 7 Ldb19, Rod1, and Rog3 bind preferentially to the C-terminal tail of Ste2. (A, lower) GST and GST-Ste2(297-431) (the tail), which was constructed, expressed in *E. coli*, and purified to apparent homogeneity as described previously (21), were used to coat glutathione-agarose beads to an equivalent level. (Upper) In this representative experiment, samples of the beads were incubated in duplicate with equivalent amounts (cpm) of [^{35}S]Met-labeled molecules of the indicated α-arrestins (pink dots) and prepared by coupled *in vitro* transcription and translation. The amount of bound radioactive protein detected was quantified using a phosphorimager as described in Materials and Methods. (B) Average fold increase in the level of radioactivity bound to the GST-Ste2^{tail} construct relative to that bound to the GST control for the indicated α-arrestins in independent replicates (*n* = 3), each performed essentially as described for panel A. Error bars indicate ±SEM. The dashed line indicates behavior expected for a negative control [i.e., no increase in binding to GST-Ste2(297-431) compared to that of GST alone, yielding a ratio of 1]. (C) Same as described for panel A, except that binding of *in vitro*-transcribed and -translated Rog3 and Rog3^{Δ400} are compared. (D) The average fold increase in binding, determined in panel B for independent replicates (*n* = 3), each performed as described for panel C.

we found that Rog3(Δ400-733) retained the ability to bind to the Ste2 cytosolic tail (Fig. 7C and D). Thus, Ldb19, Rod1, and Rog3 fulfill all of the requirements of adaptors for the downregulation, modification, and endocytosis of Ste2; they associate specifically with Rsp5, bind preferentially to the C-terminal tail of Ste2, and reduce Ste2 abundance at the cell surface.

Rod1 must be dephosphorylated by calcineurin to promote signal desensitization. Endocytosis of PM nutrient transporters is regulated by metabolic conditions. For example, under glucose-replete conditions, the lactate transporter Jen1 is internalized in a Rod1- and Rsp5-dependent manner (102). Upon glucose limitation, however, Snf1 (yeast AMPK) is activated (112) and phosphorylates Rod1 (113), inhibiting its function. This event allows Jen1 to accumulate in the PM (102). Similarly, we noted during the course of our studies that overexpression of Rod1 on galactose medium, another condition under which Snf1 is active (112), failed to promote adaptation of *sst2*Δ cells (data not shown). These data suggest that Rod1 phosphorylation blocks its association with Ste2. Glc7 (yeast phosphoprotein phosphatase 1) bound to targeting subunit Reg1 has been implicated in the dephosphorylation of

Rod1 required for Jen1 internalization (102). For several reasons, we suspected that the role of Rod1 in promoting pheromone signal desensitization is a feedback mechanism that requires dephosphorylation controlled by Ca^{2+} and the Ca^{2+}-activated phosphatase CN (yeast phosphoprotein phosphatase 2B). First, elevated Ca^{2+} influx is a consequence of pheromone action (114). Second, we showed previously that optimal CN function is required for efficient adaptation after *MAT***a** cells are exposed to α-factor (115). Third, we demonstrated recently that CN-mediated dephosphorylation of another α-arrestin, Aly1, is required to promote endocytosis of the aspartate and glutamate transporter Dip5 (78). Finally, like Aly1, Rod1 was identified in a global screen for CN substrates and found to be efficiently dephosphorylated by CN *in vitro* (116).

CN is recruited to substrates that contain a conserved docking motif, i.e., PXIXIT and variants thereof (117). Indeed, compared to a GST control, a GFP-tagged derivative of the CN catalytic subunit Cna1 copurified with GST-Rod1 from yeast extracts, whereas an equivalent level of GST-Rod1^{AQAKAA} (in which the sole PXIXIT motif, ^{545}PQIKIE^{550}, was mutated) exhibited a dra-

matic decrease (>90%) in the amount of Cna1-GFP recovered (Fig. 8A). Consistent with this site being required for efficient CN-dependent dephosphorylation *in vivo*, we found that GST-Rod1^{AQAKAA} resolved into two bands in cells in which CN was activated by exposure to 200 mM CaCl$_2$, whereas GST-Rod1 migrated as a single band (Fig. 8B, upper). The GST-Rod1^{AQAKAA}-derived species were clearly phosphorylated, because they collapsed to a single faster-mobility band upon treatment with λ phosphatase (Fig. 8B, upper). Likewise, GST-Rod1 also migrated as two distinct bands when the cells were treated with the potent CN-specific inhibitor FK506 (Fig. 8B, upper) or in mutants lacking either the Ca^{2+}-binding regulatory subunit (Cnb1) of CN (Fig. 8B, middle) or both of its catalytic subunit isoforms (Cna1 and Cna2) (Fig. 8B, lower). These GST-Rod1-derived bands co-migrated with those observed for GST-Rod1^{AQAKAA}. These species also collapsed to the same single faster-mobility species after λ phosphatase treatment (Fig. 8B). These findings demonstrate that efficient dephosphorylation of Rod1 *in vivo* requires CN action.

In agreement with the conclusion that phosphorylation of Rod1 at these CN-sensitive sites blocks its ability to promote desensitization after pheromone response, we observed less turbid halos in the adaptation assay when GST-Rod1^{AQAKAA} was overexpressed in *sst2Δ* cells than with GST-Rod1 (Fig. 8C). Most tellingly, in cells lacking functional CN (either *cnb1Δ* or *cna1Δ cna2Δ* mutants), overexpression of GST-Rod1 was unable to promote any detectable adaptation (Fig. 8D). In contrast, adaptation promoted by GST-Rog3 remained unaffected (Fig. 8D), even though GST-Rod1 and GST-Rog3 were expressed at an equivalent level in both wild-type cells and the CN-deficient mutants (Fig. 8E). We conclude that dephosphorylation mediated by the Ca^{2+}-dependent phosphatase CN is essential for Rod1 to downregulate pheromone signaling.

DISCUSSION

It has been presumed that the ligand-induced phosphorylation (37, 38) and Rsp5-dependent ubiquitinylation of multiple Lys residues (41, 42, 55) in the C-terminal cytosolic tail of Ste2, and the ensuing increased rate of receptor endocytosis (33, 34), contributes to signal dampening and recovery from pheromone response. Consistent with this notion, truncations that eliminate the C-terminal tail of Ste2 prevent receptor internalization and result in increased pheromone sensitivity and marked prolongation of pheromone-imposed G$_1$ arrest (37, 118). However, we now know that the C-terminal tail of Ste2 is also the primary binding site for the RGS protein Sst2; thus, it is required for efficient PM recruitment and function of Sst2 in deactivation of GTP-bound Gpa1 (21). Moreover, absence of Sst2 results in an elevation in pheromone sensitivity and in a sustained pheromone response quite similar to that conferred by receptor C-terminal truncations (37, 118), raising the formal possibility that, compared to its role in tethering Sst2 in the vicinity of its substrate, the C-terminal tail-dependent endocytosis of Ste2 *per se* has little or no function in postpheromone adaptation. Contrary to that viewpoint, the effects of an *sst2Δ* mutation and receptor truncation are somewhat additive, and high-level overexpression of *SST2* can promote recovery of tail-less Ste2 mutants from the effects of pheromone (37, 118).

The findings we describe here support the conclusion that Rsp5-dependent modification and internalization of the receptor contribute to the overall desensitization process. In addition to its

role in recovery from pheromone, receptor endocytosis may contribute to generating the receptor distribution for the polarized chemotropic growth that occurs during mating (51). Most importantly, our work answers previously unresolved questions about how Ste2 is recognized by Rsp5 to promote both its basal and ligand-induced endocytosis. Given that Rsp5 associates with the PM via its N-terminal lipid-binding C2 domain (119) but interacts with the substrates it modifies via the binding of its three tandem WW domains (103) to PPXY motifs in those targets (57, 120), it was a conundrum as to how Rsp5 recognized Ste2 as a substrate, since this receptor lacks any sequence elements resembling PPXY. The discovery that members of the α-arrestin family of adaptor proteins serve as intermediaries to recruit Rsp5 to nutrient permeases that also lack endogenous PPXY motifs suggested that members of the α-arrestin class of proteins function as the molecular matchmakers for delivering Rsp5 to Ste2.

Indeed, as documented here, three of the 14 known yeast α-arrestins contribute to signal downregulation at the receptor level, as judged by multiple independent criteria. First, lack of either Ldb19 or the paralogous pair Rod1 and Rog3 increases pheromone sensitivity, even in cells that possess all of the other demonstrated mechanisms for recovery from pheromone response. Second, simultaneous absence of Ldb19, Rod1, and Rog3 results in even greater pheromone sensitivity, comparable to that of a cell in which 9 α-arrestins (including Ldb19, Rod1, and Rog3) are absent. Third, among all of the α-arrestins tested, only Rod1, Rog3, and Ldb19 exhibited preferential binding to the site of Rsp5-dependent modification in Ste2, its cytosolic C-terminal tail. Phosphorylation of purified GST-Ste2^{tail} with recombinant casein kinase I neither enhanced nor inhibited binding of Ldb19, Rod1, or Rog3 (A. F. O'Donnell, unpublished results), indicating that, rather than creating epitopes for recruitment of these adaptors, phosphorylation simply assists in locking the tail in a solvent-accessible state after it is exposed by the pheromone-induced change in receptor conformation. Fourth, in cells expressing fluorescent derivatives of Ste2, PM accumulation of the receptor occurred in *ldb19Δ* cells, in *rod1Δ rog3Δ* cells, and especially in *ldb19Δ rod1Δ rog3Δ* (and *9arrΔ*) cells, and it was not observed in control cells or in any other single or multiple α-arrestin deletion mutants.

The bulk of either mCherry- or eGFP-tagged Ste2 resided in the vacuole under all circumstances. This behavior suggests that a large fraction of these chimeras can be recognized as incorrectly folded (and/or improperly glycosylated) and shunted to the vacuole via the Golgi body-to-endosome quality-control pathway (121, 122) more efficiently than they are delivered from the Golgi compartment to the PM. Therefore, the amount of these fluorescently tagged proteins that is properly folded and inserted into the PM may be a minority of the total synthesized. Moreover, the Golgi body-to-endosome shunt is known to depend on decoration of cargo by ubiquitin (123), making it problematic to analyze the change in modification state of our Ste2 constructs due solely to the presence or absence of Ldb19 and/or Rod1 and Rog3. Nevertheless, the observed increase in the amount of tagged Ste2 at the PM in *ldb19Δ*, *rod1Δ rog3Δ*, and *ldb19Δ rod1Δ rog3Δ* cells is consistent with their role in mediating the Rsp5-dependent endocytosis of the receptor.

Our results also show that the three α-arrestins contribute to Ste2 downregulation in discrete ways (Fig. 9). First, although paralogs Rod1 and Rog3 may have some overlapping role (be-
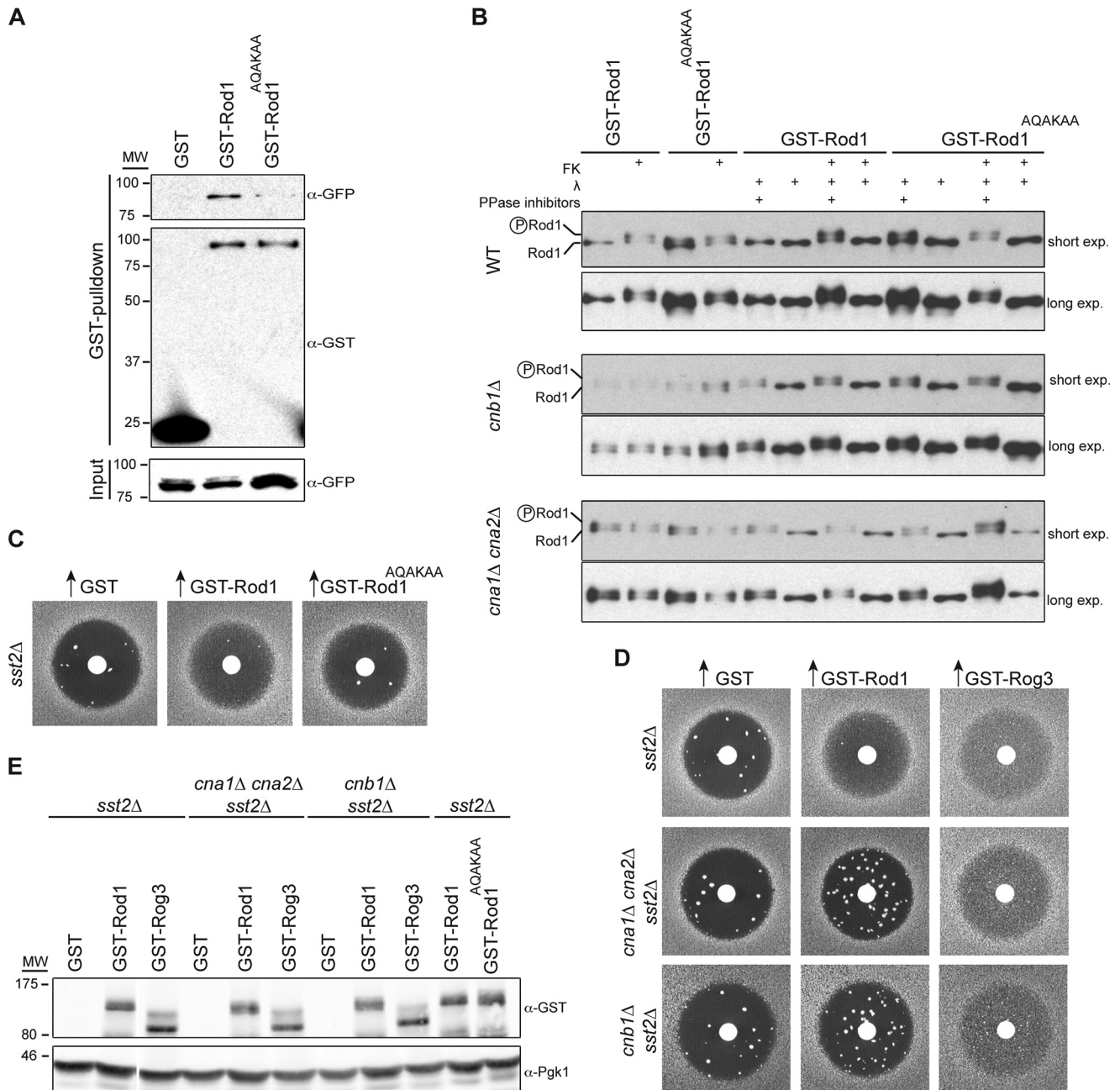
FIG 8 Rod1-mediated desensitization requires calcineurin-dependent dephosphorylation. (A) A single PXIXIT motif mediates CN-Rod1 interaction. Cultures of strain JRY11, which produces Cna1-GFP from the native *CNA1* promoter at the endogenous *CNA1* locus on chromosome XII, and also expressing, as indicated, either GST alone, GST-Rod1, or GST-Rod1^AQAKAA, were grown to mid-exponential phase, harvested, and lysed, and proteins in the resulting extracts were captured on glutathione-agarose beads, resolved by SDS-PAGE, and analyzed with the indicated antibodies. MW, molecular weight in thousands. (B) Rod1 is phosphorylated at CN-sensitive sites. Cultures of strain BY4741 (WT) or otherwise isogenic *cnb1Δ* (BY4741 *cnb1Δ*) and *cna1Δ cna2Δ* (JT5574) derivatives, as indicated, expressing either GST-Rod1 or GST-Rod1^AQAKAA were grown to mid-exponential phase and stimulated with 200 mM CaCl₂ to activate CN in either the absence or presence (+) of the CN inhibitor FK506 (FK). After harvesting and lysis, proteins in the resulting extracts were purified by capture on glutathione-agarose beads (lanes 1 to 4). Samples of the material shown in lanes 1 to 4 then were either left untreated treated or were treated (+) with lambda phosphatase (λ) in either the absence or presence (+) of phosphatase inhibitors (PPase inhibitors), and the resulting products were separated under SDS-PAGE conditions that permit resolution of phospho-isoforms and analyzed with anti-GST antibodies. exp., exposure. (C) Lack of CN binding reduces Rod1-mediated adaptation. Pheromone sensitivity of *MAT***a** *sst2Δ GEV* (JT5919) cells expressing either GST-Rod1 or GST-Rod1^AQAKAA, as indicated, under the *GAL* promoter on a high-copy-number *URA3*-marked 2μm DNA plasmid was determined as described for Fig. 1E. Data from one representative experiment (*n* = 3) are shown. (D) Absence of CN eliminates Rod1-mediated adaptation but not Rog3-mediated adaptation. Pheromone sensitivity of cultures of *MAT***a** *sst2Δ GEV* (JT5919) cells and isogenic *cnb1Δ* (JT6694) and *cna1Δ cna2Δ* (JT6695) derivatives, as indicated, expressing either GST-Rod1 or GST-Rog3 under the *GAL* promoter on a high-copy-number *URA3*-marked 2μm DNA plasmid was determined as described for Fig. 1E. Data from one representative experiment (*n* = 3) are shown. (E) Confirmation of protein expression. Whole-cell extracts of the cells used in panels C and D were prepared, resolved by SDS-PAGE, and analyzed by immunoblotting with the indicated antibodies. Here, phospho-isoforms were not separated, because different SDS-PAGE conditions were used. Data from one representative experiment (*n* = 3) are shown.
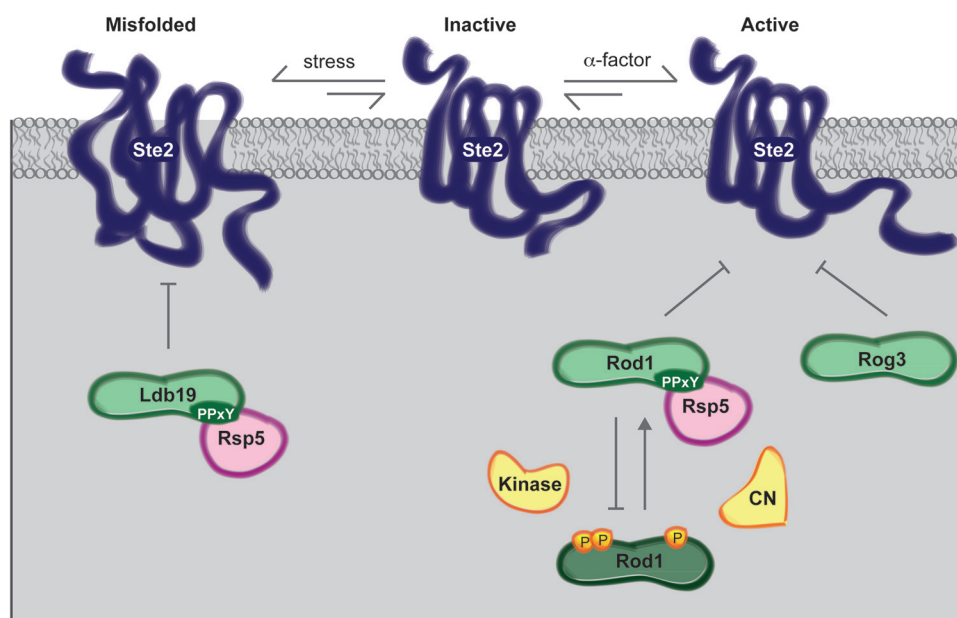
FIG 9 Distinct mechanisms of Ste2 downregulation by the α-arrestins Ldb19, Rod1, and Rog3. The α-factor receptor (Ste2), a polytopic integral membrane protein, exists primarily in three conformational states. In näive cells, Ste2 undergoes spontaneous stochastic dissociation from its cognate heterotrimeric G protein (not shown for clarity) at a certain rate and thereby becomes destabilized. When it does so, it may misfold. Current evidence suggests that Ldb19/Art1 has a primary role in a PM quality-control pathway that mediates Rsp5-dependent ubiquitinylation and endocytic removal of such misfolded PM proteins. In the presence of α-factor, Ste2 undergoes a ligand-induced conformational change that activates and dissociates its cognate G protein; however, in this case, the receptor is stabilized by bound pheromone. Because Rog3-imposed inhibition of pheromone signaling does not obligatorily require its association with or modification by Rsp5, it may act similarly to classical arrestin or β-arrestin by binding to the C-terminal tail of the receptor and sterically preventing additional rounds of G-protein activation by the pheromone-bound receptor. Later during response to pheromone, Ca^{2+} influx will stimulate the CN-dependent dephosphorylation of Rod1, making Rod1 competent to mediate Rsp5-dependent ubiquitinylation and endocytic removal of the pheromone-bound receptor, a prime example of a stimulus-induced, late-stage, negative-feedback control.

cause a detectable phenotype was found only for the *rod1Δ rog3Δ* double mutant), the loss of Ldb19 and absence of Rod1 and Rog3 had additive effects. Second, like Ldb19, the ability of Rod1 to promote adaptation requires Rsp5 binding, whereas the function of Rog3 in adaptation does not. Third, in the absence of CN-dependent dephosphorylation, Rod1 is unable to promote adaptation, whereas Rog3 is not subject to CN-mediated regulation. The most parsimonious interpretation of our collective findings is that the three different α-arrestins act on different states of the receptor and do so under different conditions (Fig. 9).

Once inserted into the PM, Ste2, like any GPCR, will exist primarily in three conformational states. Even in the absence of pheromone stimulation, Ste2 undergoes spontaneous dissociation from its cognate heterotrimeric G protein. In the absence of the stabilization conferred by receptor-G-protein interaction, Ste2 can misfold. It was shown recently that Ldb19/Art1 is essential for the Rsp5-dependent ubiquitinylation and internalization of the lysine permease Lyp1, but only after it had been subjected to heat stress (124). Thus, in the same way, the effects we observed in *ldb19Δ* cells may be explained if Ldb19 has a similar role in PM quality control in that it mediates Rsp5-dependent ubiquitinylation and endocytic removal only of misfolded Ste2. Consistent with this view, Ldb19 bound less avidly than did either Rod1 or Rog3 to the isolated Ste2 tail *in vitro*, presumably because Ldb19 recognizes an additional determinant only accessible in a misfolded receptor. For example, because native Ste2 functions as a dimer (125–127), perhaps Ldb19 associates with the tail and also a site exposed in a monomer when the dimer dissociates. In any

event, a role in removal of misfolded molecules may explain why overexpression of Ldb19 was unable to enhance the rate of recovery in the adaptation assay, which is conducted under conditions where the properly folded state of the receptor is stabilized by ligand binding. In the absence of Ldb19, unfolded receptor is not removed from the cell surface, explaining the increase in Ste2-mCherry and Ste2-GFP observed in *ldb19Δ* cells. Moreover, since misfolded receptor is not removed from *ldb19Δ* cells, it has a chance to refold and recouple to the G protein, raising the concentration of receptor competent for signaling in the first place and explaining the modest increase in pheromone sensitivity displayed by *ldb19Δ* cells.

When *MAT*a cells are exposed to α-factor, Ste2 undergoes a ligand-induced conformational change that activates and dissociates its cognate G protein; however, in contrast to when the G protein stochastically dissociates from the näive receptor in untreated cells, activated receptor is stabilized by bound pheromone. Because Rog3 potently stimulates desensitization and does not obligatorily require its association with or modification by Rsp5 to do so, it may act in a manner similar to that of retinal arrestin or β-arrestin (128). Specifically, by binding to the C-terminal tail of the receptor, Rog3 may sterically prevent the pheromone-bound receptor from catalyzing additional rounds of G-protein activation. Indeed, just like mammalian arrestin and β-arrestin, which lack PPXY motifs and have no long C-terminal extension (59, 60), the arrestin fold domain at the N terminus of Rog3 is sufficient to promote adaptation. Although technically challenging, it will be important to determine in future experiments whether Rog3

competes with Gpa1 for receptor binding. Alternatively, Rog3 may promote the clathrin- and Sla1-dependent, but ubiquitin-independent, route of endocytosis that has been defined for membrane proteins that contain an exposed NPFx$_{1-2}$D motif (129–131). Ste2 contains a very similar sequence, ^{392}GPFAD^{396}, in its C-terminal tail. On the other hand, although Rog3 does not need to recruit Rsp5 to execute its role in squelching pheromone signaling, it does possess P/VPXY motifs competent to bind Rsp5. Hence, normally, Rog3 may both interfere with receptor-G-protein recoupling and mediate Rsp5-dependent ubiquitinylation, thereby enhancing the efficiency of Ste2 capture by the components of the endocytic machinery that recognize ubiquitinylated cargo (132). This dual function may explain why Rog3 appears more efficacious than Rod1 in promoting adaptation when overexpressed. Moreover, Ste2 is the first target of Rog3 identified.

Our results indicate that Rod1 is a component of a negative feedback loop that ensures complete receptor clearance after a *MAT*a cell has committed to a productive pheromone response. One hallmark of the later stages of pheromone response is a robust influx of Ca^{2+} (133, 134). This rise in intracellular Ca^{2+} is sufficient to activate the Ca^{2+}-dependent phosphatase calcineurin (135). As we have demonstrated here, CN-mediated dephosphorylation makes Rod1 competent to stimulate adaptation after *MAT*a cells are exposed to α-factor (Fig. 9). In contrast, loss of CN activity did not prevent Rog3-promoted adaptation to pheromone, demonstrating that regulation by CN is specific to Rod1. Indeed, the PXIXIT motif in Rod1 is not conserved in Rog3. Along with Aly1 (78), Rod1 is now the second yeast α-arrestin shown to be under CN regulation. Also, in *Caenorhabditis elegans*, the function of α-arrestin CNP-1/ArrD-17 requires CN-mediated dephosphorylation (136), suggesting that CN control of α-arrestin dephosphorylation is a conserved regulatory mechanism.

Snf1 negatively regulates Rod1 function in response to glucose limitation, thereby preventing endocytosis of the lactate permease Jen1 (102, 113). Similarly, AMPK phosphorylates and promotes degradation of the mammalian α-arrestin family member TXNIP, thereby increasing glucose uptake by preventing TXNIP-mediated downregulation of the glucose transporter GLUT1 (137). Moreover, in glucose control of Rod1 action on Jen1, Reg1-bound Glc7 seems to be responsible for Rod1 dephosphorylation (64) and likely also prevents Snf1-mediated phosphorylation of Rod1 by deactivating Snf1 itself (138). However, we observed a requirement for CN-dependent dephosphorylation for Rod1 action on Ste2 on glucose-rich medium, a condition under which Snf1 is not activated (112). These observations raised two important points. First, Snf1 cannot be the only protein kinase responsible for phosphorylating and inhibiting Rod1. In fact, phosphorylation seems to be a general mechanism for blocking the endocytic action of other α-arrestin family members (78, 108, 139). Second, it is clear, at least in the case of Rod1, that the same α-arrestin is being subjected to differential phospho-regulation as a means to control endocytosis of different targets in response to distinct stimuli.

Previous reports provide evidence that ubiquitinylation of Ldb19 (57) and Rod1 (102) is necessary for their function in internalizing other cargoes. We found, however, that ubiquitinylation of Ldb19, Rod1, and Rog3 themselves was dispensable for negative regulation of Ste2-initiated signaling. Moreover, compared to the wild-type proteins, we observed only modest increases in the steady-state level of nonubiquitinylatable (PPXY-less and K-to-R) variants of these three α-arrestins, suggesting

that their Rsp5-mediated modification does not trigger rapid proteasome-mediated degradation. Indeed, Rsp5 is known to install K63-linked polyubiquitin chains on target Lys residues (140), and binding of accessory proteins, such as ESCRT-0 (141) and ESCRT-1 (109), blocks K63-linked chain recognition by proteasomes (141) or K63-linked chain formation on substrates (142). Moreover, paring back of the K63-linked chains by cellular deubiquitinylating enzymes leaves monoubiquitinylated Lys residues (143), which are poorly recognized by the proteasome (144). Although ubiquitinylation of Ldb19, Rod1, and Rog3 is not required for their function, decoration with ubiquitin might prevent Rsp5 binding. If so, ubiquitinylation of these α-arrestins themselves would provide a built-in delay timer that, after an appropriate extent of modification, eventually dissociates Rsp5 and thereby recycles this E3. Alternatively, like phosphorylation, ubiquitinylation may be yet another means to control differentially the interaction of the same α-arrestin with different targets in response to discrete signals.

Presumably, defects in *LDB19*, and especially in *ROD1* and *ROG3*, were not identified in standard screens for loss-of-function mutations that confer elevated pheromone sensitivity because of their overlapping functions. Indeed, in the case of *ROD1* and *ROG3*, we observed a detectable phenotype only in the *rod1Δ rog3Δ* double mutant. One reason the effects of these mutations appears modest is that the level of these α-arrestins is quite low (Ldb19, 295 per cell; Rod1, 386 per cell [Rog3 was not reported] [145]) compared to the number of receptors on the surface of a *MAT*a cell, ~8,000 per cell (32, 125, 146). Thus, this difference in stoichiometry may explain why it has been technically difficult to observe colocalization of these molecules with Ste2 under normal cellular conditions (C. Alvaro, unpublished observations). In contrast, colocalization of the much more abundant Sst2 (5,980 molecules per cell [145]) with Ste2 was readily observed (21). Indeed, colocalization of Ldb19 (57) and Rod1 (102) with their respective cargoes has not been demonstrated, even when overexpressed (C. Alvaro, unpublished observations), perhaps indicating the transient nature of α-arrestin-target interaction. Nonetheless, when the quantity of either Rod1 or Rog3 was elevated, the adaptation assay revealed that the ability of these α-arrestins to squelch signaling by the ligand-bound form of the receptor is actually quite potent.

In addition to Ste2, it is formally possible that Ldb19, Rod1, and/or Rog3 mediates the Rsp5-dependent modification of other factors that might lead to downregulation of a pheromone-induced signal. One study indicates that the Gα subunit (Gpa1) of the Ste2-associated heterotrimeric G protein undergoes Rsp5-mediated mono- and polyubiquitinylation, which reportedly downregulates the amount of Gpa1 at the PM by diverting it to the vacuole or to the proteasome, respectively (147). Because Gpa1 holds the Gβγ (Ste4-Ste18) complex in check and prevents signal propagation, loss of any factor that contributes to Rsp5-dependent modification of Gpa1 would stabilize Gpa1, increase Gpa1 abundance at the PM, and make cells less sensitive to pheromone. Hence, Ldb19, Rod1, and Rog3 cannot be involved in the reported Rsp5-dependent modification of Gpa1, because as we have documented here, loss of these α-arrestins makes cells more sensitive to pheromone action. Similarly, it has been noted that Ste4 (Gβ) becomes ubiquitinylated in an Rsp5-dependent manner on Lys340, but the presence or absence of this modification does not affect the rate of turnover of Ste4 and, unlike loss of Ldb19, Rod1,

and Rog3, does not affect the magnitude or duration of phero-mone-induced Fus3 activation ([148]). Hence, Ldb19, Rod1, and Rog3 cannot negatively regulate pheromone responses by being responsible for mediating the reported Rsp5-dependent modification of Ste4.

Taken together, our findings indicate that, in *S. cerevisiae*, α-arrestins Rod1, Rog3, and Ldb19 are negative regulators of the α-factor receptor (Ste2) in *MAT**a*** cells. In yeast, there are other GPCRs, including the **a**-factor receptor (Ste3) in *MATα* cells ([149]), an apparent glucose sensor (Gpr1) ([150]), and an alkaline pH sensor (Rim21) ([109]). It will be important to determine which α-arrestins regulate these GPCRs and whether, as observed for nutrient permeases ([58], [124]), there is both specificity and redundancy in which α-arrestins modulate these targets, as we have found for Ste2.

Since the time we first reported our initial observations about the apparent functions of Ldb19, Rod1, and Rog3 in contributing to downregulation of GPCR-initiated signaling in yeast ([151]), members of the α-arrestin family in animal cells have been implicated in interacting with, modifying, and/or promoting the desensitization and endocytosis of several classes of GPCRs ([61], [152–155]). However, it has been reported previously that β-arrestins fulfill this role ([156], [157]); furthermore, the molecular mechanisms by which mammalian α-arrestins may contribute to downregulation of GPCR signaling is currently in dispute ([152], [154]). Because *S. cerevisiae* lacks any β-arrestin homolog, our results indicate that α-arrestins alone are capable of promoting GPCR internalization. Thus, our studies in a model organism have helped to resolve an important biological question. Therefore, α-arrestin-mediated downregulation of GPCR-initiated signaling is likely a conserved regulatory mechanism in eukaryotes. In *S. cerevisiae*, there are currently 14 documented α-arrestin members ([60], [108], [158]), whereas, to date, only eight (ArrDC1 to ArrDC5, TXNIP, and possibly DSCR3 and RGP1) are recognized in animal cells ([159]). Moreover, the number of mammalian GPCRs is very large. Hence, it is highly likely that many more mammalian α-arrestins remain to be identified and characterized and their targets delineated.

REFERENCES

1. **Granier S, Kobilka BK.** 2012. A new era of GPCR structural and chemical biology. Nat. Chem. Biol. **8**:670–673. http://dx.doi.org/10.1038/nchembio.1025.

2. **Katritch V, Cherezov V, Stevens RC.** 2013. Structure-function of the G protein-coupled receptor superfamily. Annu. Rev. Pharmacol. Toxicol. **53**:531–556. http://dx.doi.org/10.1146/annurev-pharmtox-032112-135923.

3. **Shoichet BK, Kobilka BK.** 2012. Structure-based drug screening for G-protein-coupled receptors. Trends Pharmacol. Sci. **33**:268–272. http://dx.doi.org/10.1016/j.tips.2012.03.007.

4. **Garland SL.** 2013. Are GPCRs still a source of new targets? J. Biomol. Screen. **18**:947–966. http://dx.doi.org/10.1177/1087057113498418.

5. **Gainetdinov RR, Premont RT, Bohn LM, Lefkowitz RJ, Caron MG.** 2004. Desensitization of G protein-coupled receptors and neuronal functions. Annu. Rev. Neurosci. **27**:107–144. http://dx.doi.org/10.1146/annurev.neuro.27.070203.144206.

6. **Kelly E, Bailey CP, Henderson G.** 2008. Agonist-selective mechanisms of GPCR desensitization. Br. J. Pharmacol. **153**(Suppl 1):S379–S388. http://dx.doi.org/10.1038/sj.bjp.0707604.

7. **Sprague GF, Jr, Thorner JW.** 1992. Pheromone response and signal transduction during the mating process of *Saccharomyces cerevisiae*, p 657–744. *In* Broach JR, Pringle JR, Jones EW (ed), The molecular and cellular biology of the yeast Saccharomyces: gene expression, vol 2. Cold Spring Harbor Laboratory Press, Cold Spring Harbor, NY.

8. **Bardwell L.** 2005. A walk-through of the yeast mating pheromone response pathway. Peptides **26**:339–350. http://dx.doi.org/10.1016/j.peptides.2004.10.002.

9. **Slessareva JE, Dohlman HG.** 2006. G protein signaling in yeast: new components, new connections, new compartments. Science **314**:1412–1413. http://dx.doi.org/10.1126/science.1134041.

10. **Dohlman HG, Thorner JW.** 2001. Regulation of G protein-initiated signal transduction in yeast: paradigms and principles. Annu. Rev. Biochem. **70**:703–754. http://dx.doi.org/10.1146/annurev.biochem.70.1.703.

11. **Thorner J.** 2006. Signal transduction, p 193–210. *In* Linder P, Shore D, Hall MN (ed), Landmark papers in yeast biology. Cold Spring Harbor Laboratory Press, Cold Spring Harbor, NY.

12. **Chen RE, Thorner J.** 2007. Function and regulation in MAPK signaling pathways: lessons learned from the yeast *Saccharomyces cerevisiae*. Biochim. Biophys. Acta **1773**:1311–1340. http://dx.doi.org/10.1016/j.bbamcr.2007.05.003.

13. **Yu RC, Resnekov O, Abola AP, Andrews SS, Benjamin KR, Bruck J, Burbulis IE, Colman-Lerner A, Endy D, Gordon A, Holl M, Lok L, Pesce CG, Serra E, Smith RD, Thomson TM, Tsong AE, Brent R.** 2008. The Alpha project: a model system for systems biology research. IET Syst. Biol. **2**:222–233. http://dx.doi.org/10.1049/iet-syb:20080127.

14. **Zhang NN, Dudgeon DD, Paliwal S, Levchenko A, Grote E, Cunningham KW.** 2006. Multiple signaling pathways regulate yeast cell death during the response to mating pheromones. Mol. Biol. Cell **17**:3409–3422. http://dx.doi.org/10.1091/mbc.E06-03-0177.

15. **Doi K, Gartner A, Ammerer G, Errede B, Shinkawa H, Sugimoto K, Matsumoto K.** 1994. MSG5, a novel protein phosphatase promotes adaptation to pheromone response in *S. cerevisiae*. EMBO J. **13**:61-70.

16. **Zhan XL, Deschenes RJ, Guan KL.** 1997. Differential regulation of FUS3 MAP kinase by tyrosine-specific phosphatases PTP2/PTP3 and dual-specificity phosphatase MSG5 in *Saccharomyces cerevisiae*. Genes Dev. **11**:1690–1702. http://dx.doi.org/10.1101/gad.11.13.1690.

17. **Ciejek E, Thorner J.** 1979. Recovery of *S. cerevisiae* a cells from G1 arrest by alpha-factor pheromone requires endopeptidase action. Cell **18**:623–635. http://dx.doi.org/10.1016/0092-8674(79)90117-X.

18. **MacKay VL, Welch SK, Insley MY, Manney TR, Holly J, Saari GC, Parker ML.** 1988. The *Saccharomyces cerevisiae BAR1* gene encodes an exported protein with homology to pepsin. Proc. Natl. Acad. Sci. U. S. A. **85**:55–59. http://dx.doi.org/10.1073/pnas.85.1.55.

19. **Chan RK, Otte CA.** 1982. Physiological characterization of *Saccharomyces cerevisiae* mutants supersensitive to G1 arrest by a-factor and alpha-factor pheromones. Mol. Cell. Biol. **2**:21–29.

20. **Dohlman HG, Song J, Ma D, Courchesne WE, Thorner J.** 1996. Sst2, a negative regulator of pheromone signaling in the yeast *Saccharomyces cerevisiae*: expression, localization, and genetic interaction and physical association with Gpa1 (the G-protein alpha subunit). Mol. Cell. Biol. **16**:5194–5209.

21. **Ballon DR, Flanary PL, Gladue DP, Konopka JB, Dohlman HG, Thorner J.** 2006. DEP-domain-mediated regulation of GPCR signaling responses. Cell **126**:1079–1093. http://dx.doi.org/10.1016/j.cell.2006.07.030.

22. **Apanovitch DM, Slep KC, Sigler PB, Dohlman HG.** 1998. Sst2 is a

GTPase-activating protein for Gpa1: purification and characterization of a cognate RGS-Galpha protein pair in yeast. Biochemistry **37**:4815–4822. http://dx.doi.org/10.1021/bi9729965.

23. **Blumer KJ, Thorner J.** 1990. Beta and gamma subunits of a yeast guanine nucleotide-binding protein are not essential for membrane association of the alpha subunit but are required for receptor coupling. Proc. Natl. Acad. Sci. U. S. A. **87**:4363–4367. http://dx.doi.org/10.1073/pnas.87.11.4363.

24. **Zhou J, Arora M, Stone DE.** 1999. The yeast pheromone-responsive G alpha protein stimulates recovery from chronic pheromone treatment by two mechanisms that are activated at distinct levels of stimulus. Cell Biochem. Biophys. **30**:193–212. http://dx.doi.org/10.1007/BF02738067.

25. **Hirschman JE, Jenness DD.** 1999. Dual lipid modification of the yeast Gγ subunit Ste18p determines membrane localization of Gβγ. Mol. Cell. Biol. **19**:7705–7711.

26. **Manahan CL, Patnana M, Blumer KJ, Linder ME.** 2000. Dual lipid modification motifs in Gα and Gγ subunits are required for full activity of the pheromone response pathway in *Saccharomyces cerevisiae*. Mol. Biol. Cell **11**:957–968. http://dx.doi.org/10.1091/mbc.11.3.957.

27. **Roberts CJ, Nelson B, Marton MJ, Stoughton R, Meyer MR, Bennett HA, He YD, Dai H, Walker W, Hughes LTR, Tyers M, Boone C, Friend SH.** 2000. Signaling and circuitry of multiple MAPK pathways revealed by a matrix of global gene expression profiles. Science **287**:873–880. http://dx.doi.org/10.1126/science.287.5454.873.

28. **Dohlman HG, Goldsmith P, Spiegel AM, Thorner J.** 1993. Pheromone action regulates G-protein alpha-subunit myristoylation in the yeast *Saccharomyces cerevisiae*. Proc. Natl. Acad. Sci. U. S. A. **90**:9688–9692. http://dx.doi.org/10.1073/pnas.90.20.9688.

29. **Song J, Hirschman J, Gunn K, Dohlman HG.** 1996. Regulation of membrane and subunit interactions by N-myristoylation of a G protein alpha subunit in yeast. J. Biol. Chem. **271**:20273–20283. http://dx.doi.org/10.1074/jbc.271.34.20273.

30. **Wolfe BL, Trejo J.** 2007. Clathrin-dependent mechanisms of G protein-coupled receptor endocytosis. Traffic **8**:462–470. http://dx.doi.org/10.1111/j.1600-0854.2007.00551.x.

31. **Sorkin A, von Zastrow M.** 2009. Endocytosis and signalling: intertwining molecular networks. Nat. Rev. Mol. Cell. Biol. **10**:609–622. http://dx.doi.org/10.1038/nrm2748.

32. **Chvatchko Y, Howald I, Riezman H.** 1986. Two yeast mutants defective in endocytosis are defective in pheromone response. Cell **46**:355–364. http://dx.doi.org/10.1016/0092-8674(86)90656-2.

33. **Jenness DD, Spatrick P.** 1986. Down-regulation of the alpha-factor pheromone receptor in *S. cerevisiae*. Cell **46**:345–353. http://dx.doi.org/10.1016/0092-8674(86)90655-0.

34. **Zanolari B, Riezman H.** 1991. Quantitation of alpha-factor internalization and response during the *Saccharomyces cerevisiae* cell cycle. Mol. Cell. Biol. **11**:5251–5258.

35. **Davis NG, Horecka JL, Sprague GF, Jr.** 1993. Cis- and trans-acting functions required for endocytosis of the yeast pheromone receptors. J. Cell Biol. **122**:53–65. http://dx.doi.org/10.1083/jcb.122.1.53.

36. **Schandel KA, Jenness DD.** 1994. Direct evidence for ligand-induced internalization of the yeast alpha-factor pheromone receptor. Mol. Cell. Biol. **14**:7245–7255.

37. **Reneke JE, Blumer KJ, Courchesne WE, Thorner J.** 1988. The carboxy-terminal segment of the yeast alpha-factor receptor is a regulatory domain. Cell **55**:221–234. http://dx.doi.org/10.1016/0092-8674(88)90045-1.

38. **Chen Q, Konopka JB.** 1996. Regulation of the G-protein-coupled alpha-factor pheromone receptor by phosphorylation. Mol. Cell. Biol. **16**:247–257.

39. **Roth AF, Davis NG.** 1996. Ubiquitination of the yeast a-factor receptor. J. Cell Biol. **134**:661–674. http://dx.doi.org/10.1083/jcb.134.3.661.

40. **Feng Y, Davis NG.** 2000. Akr1p and the type I casein kinases act prior to the ubiquitination step of yeast endocytosis: Akr1p is required for kinase localization to the plasma membrane. Mol. Cell. Biol. **20**:5350–5359. http://dx.doi.org/10.1128/MCB.20.14.5350-5359.2000.

41. **Hicke L, Zanolari B, Riezman H.** 1998. Cytoplasmic tail phosphorylation of the alpha-factor receptor is required for its ubiquitination and internalization. J. Cell Biol. **141**:349–358. http://dx.doi.org/10.1083/jcb.141.2.349.

42. **Dunn R, Hicke L.** 2001. Domains of the Rsp5 ubiquitin-protein ligase required for receptor-mediated and fluid-phase endocytosis. Mol. Biol. Cell **12**:421–435. http://dx.doi.org/10.1091/mbc.12.2.421.

43. **Katzmann DJ, Odorizzi G, Emr SD.** 2002. Receptor downregulation and multivesicular-body sorting. Nat. Rev. Mol. Cell. Biol. **3**:893–905. http://dx.doi.org/10.1038/nrm973.

44. **Stoll KE, Brzovic PS, Davis TN, Klevit RE.** 2011. The essential Ubc4/Ubc5 function in yeast is HECT E3-dependent, and RING E3-dependent pathways require only monoubiquitin transfer by Ubc4. J. Biol. Chem. **286**:15165–15170. http://dx.doi.org/10.1074/jbc.M110.203968.

45. **Kamadurai HB, Souphron J, Scott DC, Duda DM, Miller DJ, Stringer D, Piper RC, Schulman BA.** 2009. Insights into ubiquitin transfer cascades from a structure of a UbcH5B-ubiquitin-HECT^{NEDD4L} complex. Mol. Cell **36**:1095–1102. http://dx.doi.org/10.1016/j.molcel.2009.11.010.

46. **Tan PK, Davis NG, Sprague GF, Payne GS.** 1993. Clathrin facilitates the internalization of seven transmembrane segment receptors for mating pheromones in yeast. J. Cell Biol. **123**:1707–1716. http://dx.doi.org/10.1083/jcb.123.6.1707.

47. **Panek HR, Stepp JD, Engle HM, Marks KM, Tan PK, Lemmon SK, Robinson LC.** 1997. Suppressors of YCK-encoded yeast casein kinase 1 deficiency define the four subunits of a novel clathrin AP-1 complex. EMBO J. **16**:4194–4204. http://dx.doi.org/10.1093/emboj/16.14.4194.

48. **Katzmann DJ, Sarkar S, Chu T, Audhya A, Emr SD.** 2004. Multivesicular body sorting: ubiquitin ligase Rsp5 is required for the modification and sorting of carboxypeptidase S. Mol. Biol. Cell **15**:468–480. http://dx.doi.org/10.1091/mbc.E03-07-0473.

49. **Gabriely G, Kama R, Gerst JE.** 2007. Involvement of specific COPI subunits in protein sorting from the late endosome to the vacuole in yeast. Mol. Cell. Biol. **27**:526–540. http://dx.doi.org/10.1128/MCB.00577-06.

50. **Toshima JY, Toshima J, Kaksonen M, Martin AC, King DS, Drubin DG.** 2006. Spatial dynamics of receptor-mediated endocytic trafficking in budding yeast revealed by using fluorescent alpha-factor derivatives. Proc. Natl. Acad. Sci. U. S. A. **103**:5793–5798. http://dx.doi.org/10.1073/pnas.0601042103.

51. **Suchkov DV, DeFlorio R, Draper E, Ismael A, Sukumar M, Arkowitz R, Stone DE.** 2010. Polarization of the yeast pheromone receptor requires its internalization but not actin-dependent secretion. Mol. Biol. Cell **21**:1737–1752. http://dx.doi.org/10.1091/mbc.E09-08-0706.

52. **Chen L, Davis NG.** 2002. Ubiquitin-independent entry into the yeast recycling pathway. Traffic **3**:110–123. http://dx.doi.org/10.1034/j.1600-0854.2002.030204.x.

53. **Shields S, Oestreich BAJ, Winistorfer S, Nguyen D, Payne JA, Katzmann DJ, Piper RC.** 2009. ESCRT ubiquitin-binding domains function cooperatively during MVB cargo sorting. J. Cell Biol. **185**:213–224. http://dx.doi.org/10.1083/jcb.200811130.

54. **Roth AF, Davis NG.** 2000. Ubiquitination of the PEST-like endocytosis signal of the yeast a-factor receptor. J. Biol. Chem. **275**:8143–8153. http://dx.doi.org/10.1074/jbc.275.11.8143.

55. **Toshima JY, Nakanishi J, Mizuno K, Toshima J, Drubin DG.** 2009. Requirements for recruitment of a G protein-coupled receptor to clathrin-coated pits in budding yeast. Mol. Biol. Cell **20**:5039–5050. http://dx.doi.org/10.1091/mbc.E09-07-0541.

56. **Alvarez CE.** 2008. On the origins of arrestin and rhodopsin. BMC Evol. Biol. **8**:222.221–222.213. http://dx.doi.org/10.1186/1471-2148-8-222.

57. **Lin CH, MacGurn JA, Chu T, Stefan CJ, Emr SD.** 2008. Arrestin-related ubiquitin-ligase adaptors regulate endocytosis and protein turnover at the cell surface. Cell **135**:714–725. http://dx.doi.org/10.1016/j.cell.2008.09.025.

58. **Nikko E, Pelham HR.** 2009. Arrestin-mediated endocytosis of yeast plasma membrane transporters. Traffic **10**:1856–1867. http://dx.doi.org/10.1111/j.1600-0854.2009.00990.x.

59. **Hatakeyama R, Kamiya Takahara MT, Maeda T.** 2010. Endocytosis of the aspartic acid/glutamic acid transporter Dip5 is triggered by substrate-dependent recruitment of the Rsp5 ubiquitin ligase via the arrestin-like protein Aly2. Mol. Cell. Biol. **30**:5598–5607. http://dx.doi.org/10.1128/MCB.00464-10.

60. **O'Donnell AF.** 2012. The running of the Buls: control of permease trafficking by alpha-arrestins Bul1 and Bul2. Mol. Cell. Biol. **32**:4506–4509. http://dx.doi.org/10.1128/MCB.01176-12.

61. **Patwari P, Lee RT.** 2012. An expanded family of arrestins regulate metabolism. Trends Endocrinol. Metab. **23**:216–222. http://dx.doi.org/10.1016/j.tem.2012.03.003.

62. **Kühn H, Wilden U.** 1987. Deactivation of photoactivated rhodopsin by rhodopsin-kinase and arrestin. J. Recept. Res. **7**:283–298.

63. **Benovic JL, Kühn H, Weyand I, Codina J, Caron MG, Lefkowitz RJ.**

1987. Functional desensitization of the isolated beta-adrenergic receptor by the beta-adrenergic receptor kinase: potential role of an analog of the retinal protein arrestin (48-kDa protein). Proc. Natl. Acad. Sci. U. S. A. **84:**8879–8882. http://dx.doi.org/10.1073/pnas.84.24.8879.

64. **Sherman F, Fink GR, Hicks JB.** 1986. Laboratory course manual for methods in yeast genetics. Cold Spring Harbor Laboratory Press, Cold Spring Harbor, NY.

65. **Amberg DC, Burke DJ, Strathern JN.** 2005. Methods in yeast genetics. Cold Spring Harbor Laboratory, Cold Spring Harbor, NY.

66. **Green MR, Sambrook J.** 2012. Molecular cloning: a laboratory manual, vol 1. Cold Spring Harbor Laboratory Press, Cold Spring Harbor, NY.

67. **Green MR, Sambrook J.** 2012. Molecular Cloning: A Laboratory Manual, vol 2. Cold Spring Harbor Laboratory Press, Cold Spring Harbor, NY.

68. **Gao CY, Pinkham JL.** 2000. Tightly regulated, beta-estradiol dose-dependent expression system for yeast. Biotechniques **29:**1226–1231.

69. **Veatch JR, McMurray MA, Nelson ZW, Gottschling DE.** 2009. Mitochondrial dysfunction leads to nuclear genome instability via an iron-sulfur cluster defect. Cell **137:**1247–1258. http://dx.doi.org/10.1016/j.cell.2009.04.014.

70. **Volland C, Urban-Grimal D, Géraud G, Haguenauer-Tsapis R.** 1994. Endocytosis and degradation of the yeast uracil permease under adverse conditions. J. Biol. Chem. **269:**9833–9841.

71. **Westfall PJ, Patterson JC, Chen RE, Thorner J.** 2008. Stress resistance and signal fidelity independent of nuclear MAPK function. Proc. Natl. Acad. Sci. U. S. A. **105:**12212–12217. http://dx.doi.org/10.1073/pnas.0805797105.

72. **Laemmli UK.** 1970. Cleavage of structural proteins during the assembly of the head of bacteriophage T4. Nature **227:**680–685. http://dx.doi.org/10.1038/227680a0.

73. **Patterson JC, Klimenko ES, Thorner J.** 2010. Single-cell analysis reveals that insulation maintains signaling specificity between two yeast MAPK pathways with common components. Sci. Signal. **3:**ra75. http://dx.doi.org/10.1126/scisignal.2001275.

74. **Towbin H, Staehelin T, Gordon J.** 1979. Electrophoretic transfer of proteins from polyacrylamide gels to nitrocellulose sheets: procedure and some applications. Proc. Natl. Acad. Sci. U. S. A. **76:**4350–4354. http://dx.doi.org/10.1073/pnas.76.9.4350.

75. **Towbin H, Gordon J.** 1984. Immunoblotting and dot immunobinding–current status and outlook. J. Immunol. Methods **72:**313–340. http://dx.doi.org/10.1016/0022-1759(84)90001-2.

76. **Baum P, Thorner J, Honig L.** 1978. Identification of tubulin from the yeast *Saccharomyces cerevisiae*. Proc. Natl. Acad. Sci. U. S. A. **75:**4962–4966. http://dx.doi.org/10.1073/pnas.75.10.4962.

77. **Bultynck G, Heath VL, Majeed AP, Galan JM, Haguenauer-Tsapis R, Cyert MS.** 2006. Slm1 and Slm2 are novel substrates of the calcineurin phosphatase required for heat stress-induced endocytosis of the yeast uracil permease. Mol. Cell. Biol. **26:**4729–4745. http://dx.doi.org/10.1128/MCB.01973-05.

78. **O'Donnell AF, Huang L, Thorner J, Cyert MS.** 2013. A calcineurin-dependent switch controls the trafficking function of alpha-arrestin Aly1/Art6. J. Biol. Chem. **288:**24063–24080. http://dx.doi.org/10.1074/jbc.M113.478511.

79. **Kee Y, Munoz W, Lyon N, Huibregtse JM.** 2006. The deubiquitinating enzyme Ubp2 modulates Rsp5-dependent Lys63-linked polyubiquitin conjugates in *Saccharomyces cerevisiae*. J. Biol. Chem. **281:**36724–36731. http://dx.doi.org/10.1074/jbc.M608756200.

80. **Carroll CW, Morgan DO.** 2005. Enzymology of the anaphase-promoting complex. Methods Enzymol. **398:**219–230. http://dx.doi.org/10.1016/S0076-6879(05)98018-X.

81. **Enquist-Newman M, Sullivan M, Morgan DO.** 2008. Modulation of the mitotic regulatory network by APC-dependent destruction of the Cdh1 inhibitor Acm1. Mol. Cell **30:**437–446. http://dx.doi.org/10.1016/j.molcel.2008.04.004.

82. **Prosser DC, Drivas TG, Maldonado-Báez L, Wendland B.** 2011. Existence of a novel clathrin-independent endocytic pathway in yeast that depends on Rho1 and formin. J. Cell Biol. **195:**657–671. http://dx.doi.org/10.1083/jcb.201104045.

83. **Tevzadze GG, Pierce JV, Esposito RE.** 2007. Genetic evidence for a SPO1-dependent signaling pathway controlling meiotic progression in yeast. Genetics **175:**1213–1227. http://dx.doi.org/10.1534/genetics.106.069252.

84. **Brar GA, Yassour M, Friedman N, Regev A, Ingolia NT, Weissman JS.**

85. **Novoselova TV, Zahira K, Rose RS, Sullivan JA.** 2012. Bul proteins, a nonredundant, antagonistic family of ubiquitin ligase regulatory proteins. Eukaryot. Cell **11:**463–470. http://dx.doi.org/10.1128/EC.00009-12.

86. **O'Donnell AF, Apffel A, Gardner RG, Cyert MS.** 2010. Alpha-arrestins Aly1 and Aly2 regulate intracellular trafficking in response to nutrient signaling. Mol. Biol. Cell **21:**3552–3566. http://dx.doi.org/10.1091/mbc.E10-07-0636.

87. **Whiteway M, Hougan L, Thomas DY.** 1988. Expression of MFalpha1 in MATa cells supersensitive to alpha-factor leads to self-arrest. Mol. Gen. Genet. **214:**85–88. http://dx.doi.org/10.1007/BF00340184.

88. **Blackwell E, Halatek IM, Kim HJN, Ellicott AT, Obukhov AA, Stone DE.** 2003. Effect of the pheromone-responsive G and phosphatase proteins of *Saccharomyces cerevisiae* on the subcellular localization of the Fus3 mitogen-activated protein kinase. Mol. Biol. Cell. **23:**1135–1150. http://dx.doi.org/10.1128/MCB.23.4.1135-1150.2003.

89. **Elion EA, Grisafi PL, Fink GR.** 1990. FUS3 encodes a cdc2+/CDC28-related kinase required for the transition from mitosis into conjugation. Cell **60:**649–664. http://dx.doi.org/10.1016/0092-8674(90)90668-5.

90. **Boulton TG, Yancopoulous GD, Gregory JS, Slaughter C, Moomaw C, Hsu J, Cobb MH.** 1990. An insulin-stimulated protein kinase similar to yeast kinases involved in cell cycle control. Science **249:**64–67. http://dx.doi.org/10.1126/science.2164259.

91. **Bardwell L, Cook JG, Chang EC, Cairns BR, Thorner J.** 1996. Signaling in the yeast pheromone response pathway: specific and high-affinity interaction of the mitogen-activated protein (MAP) kinases Kss1 and Fus3 with the upstream MAP kinase kinase Ste7. Mol. Cell. Biol. **16:**3637–3650.

92. **Trueheart J, Boeke JD, Fink GR.** 1987. Two genes required for cell fusion during yeast conjugation: evidence for a pheromone-induced surface protein. Mol. Cell. Biol. **7:**2316–2328.

93. **Hasson MS, Blinder D, Thorner J, Jenness DD.** 1994. Mutational activation of the *STE5* gene product bypasses the requirement for G protein beta and gamma subunits in the yeast pheromone response pathway. Mol. Cell. Biol. **14:**1054–1065.

94. **Siekhaus DE, Drubin DG.** 2003. Spontaneous receptor-independent heterotrimeric G-protein signalling in an RGS mutant. Nat. Cell Biol. **5:**231–235. http://dx.doi.org/10.1038/ncb941.

95. **Myers MD, Payne GS.** 2013. Clathrin, adaptors and disease: insights from the yeast Saccharomyces cerevisiae. Front. Biosci. **18:**862–891. http://dx.doi.org/10.2741/4149.

96. **Prosser DC, Wendland B.** 2012. Conserved roles for yeast Rho1 and mammalian RhoA GTPases in clathrin-independent endocytosis. Small GTPases. **3:**229–235. http://dx.doi.org/10.4161/sgtp.21631.

97. **Walther TC, Brickner JH, Aguilar PS, Bernales S, Pantoja C, Walter P.** 2006. Eisosomes mark static sites of endocytosis. Nature **439:**998–1003. http://dx.doi.org/10.1038/nature04472.

98. **Moreira KE, Schuck S, Schrul B, Fröhlich F, Moseley JB, Walther TC, Walter P.** 2012. Seg1 controls eisosome assembly and shape. J. Cell Biol. **198:**405–420. http://dx.doi.org/10.1083/jcb.201202097.

99. **Brach T, Specht T, Kaksonen M.** 2011. Reassessment of the role of plasma membrane domains in the regulation of vesicular traffic in yeast. J. Cell Sci. **124:**328–337. http://dx.doi.org/10.1242/jcs.078519.

100. **Buser C, Drubin DG.** 2013. Ultrastructural imaging of endocytic sites in Saccharomyces cerevisiae by transmission electron microscopy and immunolabeling. Microsc. Microanal. **19:**381–392. http://dx.doi.org/10.1017/S1431927612014304.

101. **Grossmann G, Malinsky J, Stahlschmidt W, Loibl M, Weig-Meckl I, Frommer WB, Opekarová AM, Tanner W.** 2008. Plasma membrane microdomains regulate turnover of transport proteins in yeast. J. Cell Biol. **183:**1075–1088. http://dx.doi.org/10.1083/jcb.200806035.

102. **Becuwe M, Lara NVD, Gomes-Rezende J, Soares-Cunha C, Casal M, Haguenauer-Tsapis R, Vincent O, Paiva S, Léon S.** 2012. A molecular switch on an arrestin-like protein relays glucose signaling to transporter endocytosis. J. Cell Biol. **196:**247–259. http://dx.doi.org/10.1083/jcb.201109113.

103. **Sudol M, Recinos CC, Abraczinskas J, Humbert J, Farooq A.** 2005. WW or WoW: the WW domains in a union of bliss. IUBMB Life **57:**773–778. http://dx.doi.org/10.1080/15216540500389039.

104. **Gupta R, Kus B, Fladd C, Wasmuth J, Tonikian R, Sidhu S, Krogan**

NJ, Parkinson J, Rotin D. 2007. Ubiquitination screen using protein microarrays for comprehensive identification of Rsp5 substrates in yeast. Mol. Syst. Biol. 3:116. http://dx.doi.org/10.1038/msb4100159.

105. Rotin D, Kumar S. 2009. Physiological function of the HECT family of ubiquitin ligases. Nat. Rev. Mol. Cell Biol. 10:298–409. http://dx.doi.org/10.1038/nrm2690.

106. Lauwers E, Erpapazoglou Z, Haguenauer-Tsapis A, André B. 2010. The ubiquitin code of yeast permease trafficking. Trends Cell Biol. 20:196–204. http://dx.doi.org/10.1016/j.tcb.2010.01.004.

107. Reider A, Wendland B. 2011. Endocytic adaptors–social networking at the plasma membrane. J. Cell Sci. 124:1613–1622. http://dx.doi.org/10.1242/jcs.073395.

108. Merhi A, André B. 2012. Internal amino acids promote Gap1 permease ubiquitylation via TORC1/Npr1/14-3-3-dependent control of the Bul arrestin-like adaptors. Mol. Cell. Biol. 32:4510–4522. http://dx.doi.org/10.1128/MCB.00463-12.

109. Herrador A, Herranz S, Lara D, Vincent O. 2010. Recruitment of the ESCRT machinery to a putative seven-transmembrane-domain receptor is mediated by an arrestin-related protein. Mol. Cell. Biol. 30:897–907. http://dx.doi.org/10.1128/MCB.00132-09.

110. David NE, Gee M, Andersen B, Naider F, Thorner J, Stevens RC. 1997. Expression and purification of the Saccharomyces cerevisiae alpha-factor receptor (Ste2p), a 7-transmembrane-segment G protein-coupled receptor. J. Biol. Chem. 272:15553–15561. http://dx.doi.org/10.1074/jbc.272.24.15553.

111. Büküsoglu G, Jenness DD. 1996. Agonist-specific conformational changes in the yeast alpha-factor pheromone receptor. Mol. Cell. Biol. 16:4818–4823.

112. Hedbacker K, Carlson MB. 2008. Snf1/AMPK pathways in yeast. Front. Biosci. 13:2408–2420. http://dx.doi.org/10.2741/2854.

113. Shinoda J, Kikuchi Y. 2007. Rod1, an arrestin-related protein, is phosphorylated by Snf1-kinase in Saccharomyces cerevisiae. Biochem. Biophys. Res. Commun. 364:258–263. http://dx.doi.org/10.1016/j.bbrc.2007.09.134.

114. Ohsumi Y, Anraku Y. 1985. Specific induction of Ca^{2+} transport activity in MATa cells of Saccharomyces cerevisiae by a mating pheromone, alpha-factor. J. Biol. Chem. 260:10482–10486.

115. Cyert MS, Thorner J. 1992. Regulatory subunit (CNB1 gene product) of yeast Ca2+/calmodulin-dependent phosphoprotein phosphatases is required for adaptation to pheromone. Mol. Cell. Biol. 12:3460–3469.

116. Goldman AR. 2012. Global identification and functional analysis of calcineurin substrates in yeast. Ph.D. dissertation. Stanford University, Stanford, CA.

117. Roy J, Cyert MS. 2009. Cracking the phosphatase code: docking interactions determine substrate specificity. Sci. Signal. 2:re9. http://dx.doi.org/10.1126/scisignal.2100re9.

118. Konopka J, Jenness DD, Hartwell LH. 1988. The C-terminus of the S. cerevisiae alpha-pheromone receptor mediates an adaptive response to pheromone. Cell 54:609–620. http://dx.doi.org/10.1016/S0092-8674(88)80005-9.

119. Cho W, Stahelin RV. 2006. Membrane binding and subcellular targeting of C2 domains. Biochim. Biophys. Acta 1761:838–849. http://dx.doi.org/10.1016/j.bbalip.2006.06.014.

120. Sullivan JA, Lewis MJ, Nikko E, Pelham HR. 2007. Multiple interactions drive adaptor-mediated recruitment of the ubiquitin ligase rsp5 to membrane proteins in vivo and in vitro. Mol. Biol. Cell 18:2429–2440. http://dx.doi.org/10.1091/mbc.E07-01-0011.

121. Reggiori F, Black MW, Pelham HR. 2000. Polar transmembrane domains target proteins to the interior of the yeast vacuole. Mol. Biol. Cell 11:3737–3749. http://dx.doi.org/10.1091/mbc.11.11.3737.

122. Pizzirusso M, Chang A. 2004. Ubiquitin-mediated targeting of a mutant plasma membrane ATPase, Pma1–7, to the endosomal/vacuolar system in yeast. Mol. Biol. Cell 15:2401–2409. http://dx.doi.org/10.1091/mbc.E03-10-0727.

123. MacGurn JA, Hsu PC, Emr SD. 2012. Ubiquitin and membrane protein turnover: from cradle to grave. Annu. Rev. Biochem. 81:231–259. http://dx.doi.org/10.1146/annurev-biochem-060210-093619.

124. Zhao Y, Macgurn JA, Liu M, Emr SD. 2013. The ART-Rsp5 ubiquitin ligase network comprises a plasma membrane quality control system that protects yeast cells from proteotoxic stress. eLife 2:e00459.00451-e00459.00418.

125. Blumer KJ, Reneke JE, Courchesne WE, Thorner J. 1988. Functional domains of a peptide hormone receptor: the alpha-factor receptor (STE2

gene product) of the yeast Saccharomyces cerevisiae. Cold Spring Harbor Symp. Quant. Biol. 53(Part 2):591–603. http://dx.doi.org/10.1101/SQB.1988.053.01.068.

126. Overton MC, Chinault SL, Blumer KJ. 2003. Oligomerization, biogenesis, and signaling is promoted by a glycophorin A-like dimerization motif in transmembrane domain 1 of a yeast G protein-coupled receptor. J. Biol. Chem. 278:49369–49377. http://dx.doi.org/10.1074/jbc.M308654200.

127. Chinault SL, Overton MC, Blumer KJ. 2004. Subunits of a yeast oligomeric G protein-coupled receptor are activated independently by agonist but function in concert to activate G protein heterotrimers. J. Biol. Chem. 279:16091–16100. http://dx.doi.org/10.1074/jbc.M311099200.

128. Lohse MJ, Andexinger S, Pitcher J, Trukawinski S, Codina J, Faure JP, Caron MG, Lefkowitz RJ. 1992. Receptor-specific desensitization with purified proteins. Kinase dependence and receptor specificity of beta-arrestin and arrestin in the beta2-adrenergic receptor and rhodopsin systems. J. Biol. Chem. 267:8558–8564.

129. Tan PK, Howard JP, Payne GS. 1996. The sequence NPFXD defines a new class of endocytosis signal in Saccharomyces cerevisiae. J. Cell Biol. 135:1789–1800. http://dx.doi.org/10.1083/jcb.135.6.1789.

130. Howard JP, Hutton JL, Olson JM, Payne GS. 2002. Sla1p serves as the targeting signal recognition factor for NPFx(1,2)D-mediated endocytosis. J. Cell Biol. 157:315–326. http://dx.doi.org/10.1083/jcb.200110027.

131. Mahadev RK, Di Pietro SM, Olson JM, Piao HL, Payne GS, Overduin M. 2007. Structure of Sla1p homology domain 1 and interaction with the NPFxD endocytic internalization motif. EMBO J. 26:1963–1971. http://dx.doi.org/10.1038/sj.emboj.7601646.

132. Dores MR, Schnell JD, Maldonado-Baez L, Wendland B, Hicke L. 2010. The function of yeast epsin and Ede1 ubiquitin-binding domains during receptor internalization. Traffic 11:151–160. http://dx.doi.org/10.1111/j.1600-0854.2009.01003.x.

133. Nakajima-Shimada J, Sakaguchi S, Anraku FITY, Iida H. 2000. Ca2+ signal is generated only once in the mating pheromone response pathway in Saccharomyces cerevisiae. Cell Struct. Funct. 25:125–131. http://dx.doi.org/10.1247/csf.25.125.

134. Martin DC, Kim H, Mackin NA, Maldonado-Báez L, Evangelista CCJ, Beaudry VG, Dudgeon DD, Naiman DG, Erdman SE, Cunningham KW. 2011. New regulators of a high affinity Ca2+ influx system revealed through a genome-wide screen in yeast. J. Biol. Chem. 286:10744–10754. http://dx.doi.org/10.1074/jbc.M110.177451.

135. Withee JL, Mulholland J, Jeng R, Cyert MS. 1997. An essential role of the yeast pheromone-induced Ca^{2+} signal is to activate calcineurin. Mol. Biol. Cell 8:263–277. http://dx.doi.org/10.1091/mbc.8.2.263.

136. Jee C, Kalichamy TWCK, Yee JZ, Song HO, Ji YJ, Lee J, Lee JI, L'Etoile ND, Ahnn J, Lee SK. 2012. CNP-1 (ARRD-17), a novel substrate of calcineurin, is critical for modulation of egg-laying and locomotion in response to food and lysine sensation in Caenorhabditis elegans. J. Mol. Biol. 417:165–178. http://dx.doi.org/10.1016/j.jmb.2012.01.012.

137. Wu N, Shaywitz BZA, Dagon Y, Tower C, Bellinger G, Shen CH, Wen J, Asara J, McGraw TE, Kahn BB, Cantley LC. 2013. AMPK-dependent degradation of TXNIP upon energy stress leads to enhanced glucose uptake via GLUT1. Mol. Cell 49:1167–1175. http://dx.doi.org/10.1016/j.molcel.2013.01.035.

138. Zhang Y, McCartney RR, Chandrashekarappa DG, Mangat S, Schmidt MC. 2011. Reg1 protein regulates phosphorylation of all three Snf1 isoforms but preferentially associates with the Gal83 isoform. Eukaryot. Cell 10:1628–1636. http://dx.doi.org/10.1128/EC.05176-11.

139. MacGurn JA, Hsu PC, Smolka MB, Emr SD. 2011. TORC1 regulates endocytosis via Npr1-mediated phosphoinhibition of a ubiquitin ligase adaptor. Cell 147:1104–1117. http://dx.doi.org/10.1016/j.cell.2011.09.054.

140. Kim HC, Huibregtse JM. 2009. Polyubiquitination by HECT E3s and the determinants of chain type specificity. Mol. Cell. Biol. 29:3307–3318. http://dx.doi.org/10.1128/MCB.00240-09.

141. Nathan JA, Kim HT, Ting L, Gygi SP, Goldberg AL. 2013. Why do cellular proteins linked to K63-polyubiquitin chains not associate with proteasomes? EMBO J. 32:552–565. http://dx.doi.org/10.1038/emboj.2012.354.

142. Herrador A, Léon S, Haguenauer-Tsapis R, Vincent O. 2013. A mechanism for protein monoubiquitination dependent on a trans-acting ubiquitin-binding domain. J. Biol. Chem. 288:16206–16211. http://dx.doi.org/10.1074/jbc.C113.452250.

143. Kee Y, Muñoz W, Lyon N, Huibregtse JM. 2006. The deubiquitinating

enzyme Ubp2 modulates Rsp5-dependent Lys63-linked polyubiquitin conjugates in *Saccharomyces cerevisiae*. J. Biol. Chem. **281:**36724–36731. http://dx.doi.org/10.1074/jbc.M608756200.

144. **Pickart CM, Cohen RE.** 2004. Proteasomes and their kin: proteases in the machine age. Nat. Rev. Mol. Cell. Biol. **5:**177–187. http://dx.doi.org/10.1038/nrm1336.

145. **Ghaemmaghami S, Huh WK, Bower K, Howson RW, Belle A, Dephoure N, O'Shea EK, Weissman JS.** 2003. Global analysis of protein expression in yeast. Nature **425:**737–741. http://dx.doi.org/10.1038/nature02046.

146. **Jenness DD, Burkholder AC, Hartwell LH.** 1986. Binding of alpha-factor pheromone to Saccharomyces cerevisiae a cells: dissociation constant and number of binding sites. Mol. Cell. Biol. **6:**318–320.

147. **Torres MP, Lee MJ, Ding F, Purbeck C, Kuhlman B, Dokholyan NV, Dohlman HG.** 2009. G protein mono-ubiquitination by the Rsp5 ubiquitin ligase. J. Biol. Chem. **284:**8940–8950. http://dx.doi.org/10.1074/jbc.M809058200.

148. **Zhu M, Torres MP, Kelley JB, Dohlman HG, Wang Y.** 2011. Pheromone- and Rsp5-dependent ubiquitination of the G protein beta subunit Ste4 in yeast. J. Biol. Chem. **286:**27147–27155. http://dx.doi.org/10.1074/jbc.M111.254193.

149. **Clark KL, Davis NG, Wiest DK, Hwang-Shum JJ, Sprague GF, Jr.** 1988. Response of yeast alpha cells to a-factor pheromone: topology of the receptor and identification of a component of the response pathway. Cold Spring Harbor Symp. Quant. Biol. **53**(Part 2):611–620. http://dx.doi.org/10.1101/SQB.1988.053.01.070.

150. **Lemaire K, Van de Velde S, Van Dijck P, Thevelein JM.** 2004. Glucose and sucrose act as agonist and mannose as antagonist ligands of the G protein-coupled receptor Gpr1 in the yeast *Saccharomyces cerevisiae*. Mol. Cell **16:**293–299. http://dx.doi.org/10.1016/j.molcel.2004.10.004.

151. **Alvaro C, O'Donnell AF, Thorner J.** 2011. The alpha-arrestins Ldb19/Art1, Rod1/Art4 and Rog3.Art7 promote basal and ligand-induced internalization of GPCR Ste2, p 25. *In* Bloom K, Cyert MS, Weisman L (ed), Abstr. Yeast Cell Biol. Meet. Cold Spring Harb. Lab. Cold Spring Harbor Laboratory Press, Cold Spring Harbor, NY.

152. **Nabhan JF, Pan H, Lu Q.** 2010. Arrestin domain-containing protein 3 recruits the NEDD4 E3 ligase to mediate ubiquitination of the beta2-adrenergic receptor. EMBO Rep. **11:**605–611. http://dx.doi.org/10.1038/embor.2010.80.

153. **Shea FF, Rowell JL, Li Y, Chang TH, Alvarez CE.** 2012. Mammalian alpha-arrestins link activated seven transmembrane receptors to Nedd4 family E3 ubiquitin ligases and interact with beta-arrestins. PLoS One **7:**e50557. http://dx.doi.org/10.1371/journal.pone.0050557.

154. **Han SO, Kommaddi RP, Shenoy SK.** 2013. Distinct roles for beta-arrestin2 and arrestin-domain-containing proteins in β2 adrenergic re-

ceptor trafficking. EMBO Rep. **14:**164–171. http://dx.doi.org/10.1038/embor.2012.187.

155. **Kwon Y, Vinayagam A, Sun X, Dephoure N, Gygi SP, Perrimon PHN.** 2013. The Hippo signaling pathway interactome. Science **342:**737–740. http://dx.doi.org/10.1126/science.1243971.

156. **Claing A, Laporte SA, Caron MG, Lefkowitz RJ.** 2002. Endocytosis of G protein-coupled receptors: roles of G protein-coupled receptor kinases and beta-arrestin proteins. Prog. Neurobiol. **66:**61–79. http://dx.doi.org/10.1016/S0301-0082(01)00023-5.

157. **Callander GE, Thomas WG, Bathgate RA.** 2009. Prolonged RXFP1 and RXFP2 signaling can be explained by poor internalization and a lack of beta-arrestin recruitment. Am. J. Physiol. Cell Physiol. **296:**C1058–C1066. http://dx.doi.org/10.1152/ajpcell.00581.2008.

158. **Becuwe M, Herrador A, Haguenauer-Tsapis R, Vincent O, Léon S.** 2012. Ubiquitin-mediated regulation of endocytosis by proteins of the arrestin family. Biochem. Res. Int. **2012:**242764. http://dx.doi.org/10.1155/2012/242764.

159. **Aubry L, Klein G.** 2013. True arrestins and arrestin-fold proteins: a structure-based appraisal. Prog. Mol. Biol. Transl. Sci. **118:**21–56. http://dx.doi.org/10.1016/B978-0-12-394440-5.00002-4.

160. **Jones EW.** 2002. Vacuolar proteases and proteolytic artifacts in *Saccharomyces cerevisiae*. Methods Enzymol. **351:**127–150. http://dx.doi.org/10.1016/S0076-6879(02)51844-9.

161. **McIsaac RS, Silverman SJ, McClean MN, Gibney PA, Macinskas J, Hickman MJ, Petti AA, Botstein D.** 2011. Fast-acting and nearly gratuitous induction of gene expression and protein depletion in *Saccharomyces cerevisiae*. Mol. Biol. Cell **22:**4447–4459. http://dx.doi.org/10.1091/mbc.E11-05-0466.

162. **Mitchell DA, Marshall TK, Deschenes RJ.** 1993. Vectors for the inducible overexpression of glutathione S-transferase fusion proteins in yeast. Yeast **9:**715–722. http://dx.doi.org/10.1002/yea.320090705.

163. **Zhu H, Klemic JF, Chang S, Bertone P, Casamayor A, Klemic KG, Smith D, Gerstein M, Reed MA, Snyder M.** 2000. Analysis of yeast protein kinases using protein chips. Nat. Genet. **26:**283–289. http://dx.doi.org/10.1038/81576.

164. **Sikorski RS, Hieter P.** 1989. A system of shuttle vectors and yeast host strains designed for efficient manipulation of DNA in *Saccharomyces cerevisiae*. Genetics **122:**19–27.

165. **Jones LV, Tukey JW.** 2000. A sensible formulation of the significance test. Psychol. Methods **5:**411–4144. http://dx.doi.org/10.1037/1082-989X.5.4.411.

166. **Kelley LA, Sternberg MJE.** 2009. Protein structure prediction on the web: a case study using the Phyre server. Nat. Protoc. **4:**363–371. http://dx.doi.org/10.1038/nprot.2009.2.